



VICTORIA UNIVERSITY
MELBOURNE AUSTRALIA

Recent advances in graphene-derived materials for biomedical waste treatment

This is the Accepted version of the following publication

Obayomi, Kehinde Shola, Lau, Sie Yon, Mayowa, Ibitogbe Enoch, Danquah, Michael K, Zhang, Jianhua, Chiong, Tung, Meunier, Louise and Rahman, Mohammad Mahmudur (2022) Recent advances in graphene-derived materials for biomedical waste treatment. *Journal of Water Process Engineering*, 51. ISSN 2214-7144

The publisher's official version can be found at
<https://www.sciencedirect.com/science/article/pii/S2214714422008844?via%3Dihub>
Note that access to this version may require subscription.

Downloaded from VU Research Repository <https://vuir.vu.edu.au/46949/>

30 **Abstract**

31 Untreated biomedical wastes discharged into water bodies, primarily by hospitals and health care
32 facilities; release a wide range of contaminants that poses danger to human health and
33 environmental sustainability. Therefore, developing sustainable and dependable treatment
34 methods for biomedical waste is a top priority. Nano-sized graphene is known to have excellent
35 unique properties including high current density, optical, mechanical, thermal conductivity, high
36 chemical stability, high surface area and chemical stability. Graphene-based nanomaterials and
37 derivatives as a result of their excellent properties have received increased attention in wastewater
38 treatment in recent years. Despite significant progress in the production of graphene at laboratory
39 scale, there is a need to focus on green large-scale graphene synthesis to pave the way for adopting
40 graphene-based technology on an industrial scale. In wastewater treatment, advanced development
41 of pure graphene on various significant functionalization exhibits excellent adsorption efficiency
42 when functionalized when compared to other alternatives. Top-down as well as bottom-up
43 approaches such as chemical vapour deposition, and chemical exfoliation among other approaches
44 can be used for graphene synthesis and functionalization. As a result, the benefits of graphene
45 oxide-based nanomaterials have been unraveled in the treatment of biomedical wastewater.
46 Adsorption and photocatalysis techniques have sparked widespread interest because they allow for
47 the environmentally friendly treatment of biomedical wastewater, and significant progress has
48 been made in recent years. This study examined the graphene synthesis method and the use of
49 graphene oxide-based nanomaterials as adsorbents and photocatalysts in the treatment of
50 biomedical waste. Furthermore, the recyclability, thermal stability, and future perspectives on the
51 directions and difficulties in graphene-based material synthesis are summarized.

52

53 **Keywords:** Graphene; Graphene synthesis; Graphene-based nanomaterials; Biomedical waste;
54 Waste treatment; Adsorption; Photocatalysis; Mechanism

55

56

57

58

59 **1. Introduction**

60 With the innovative development of advanced biomedical technology, new challenges, such as
61 biomedical waste management, are being created (Agrawal et al. 2021; Saravanan et al. 2022).
62 Biomedical wastes (BMW) are mostly generated by pharmaceutical industries, healthcare
63 facilities, medical and educational research institutions, nursing homes, and hospitals during
64 medical treatment of human and veterinary populations as presented in Fig. 1. They include
65 expired vaccines and drugs, blood products, tissues, organic fluids, radioactive waste, and
66 chemical and pharmaceutical residues. BMW may also contain chemical, surgical, pharmaceutical,
67 cytotoxic and other biological waste materials which are potentially hazardous to living organisms
68 including humans and the environment (Dash et al. 2021; Sohal et al. 2021). Inadequate BMW
69 management can have consequences, such as increasing infectious diseases, resulting from
70 groundwater contamination (Ara et al. 2022). It has been established that even trace amounts of
71 various drug residues can exist in surface, ground and even drinking water (Komal et al. 2022).
72 The remainder of drugs that undergo partial metabolism in the human body is discharged as
73 effluent into receiving water bodies. A large majority of such drugs is antibiotics of which about
74 80–90% return to the environment via excretion in their parent form due to their robust molecular
75 structure, making them to degrade naturally (Al-Jubouri et al., 2022).

76
77 Several conventional and advanced techniques, such as electrochemical treatments, filtration,
78 precipitation, membrane separation, photocatalysis, ion-exchange, reverse osmosis and
79 adsorption, have been used for treatment of antibiotics in wastewater (Khanday et al. 2019;
80 Grisales-Cifuentes et al., 2021; Qin et al., 2022). However, they still face challenges of cost-
81 effectiveness, environmental friendliness, and process efficiency from material preparation to
82 process optimization (Lee et al. 2019). Graphene and its derivatives have impacted wastewater
83 treatment and have been utilized in photocatalysis, adsorption or as an effective electrode in
84 various treatment technologies and applications (Obayomi et al., 2022; Yang et al., 2022; Han et
85 al., 2022). Adsorption have numerous advantages such as its high efficacy, low cost, and ecological
86 viability to remove organic contaminants from water (Zhu et al., 2018; Januário et al., 2022; Zhu
87 et al., 2022).

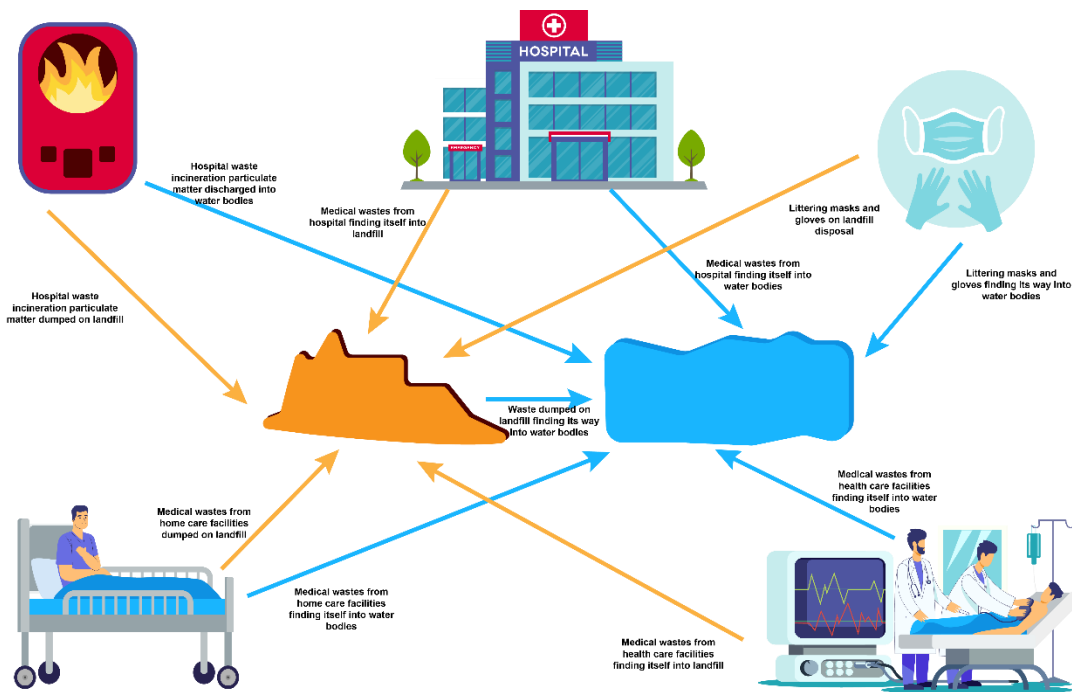


Fig. 1. Biomedical waste discharged channels into water bodies

88
89

90 Graphene is a planar single-atom layer thick sheet and two-dimensionally structured material
 91 composed of tightly packed sp^2 -bonded carbon atoms in a honeycomb crystal lattice with a distinct
 92 charge mobility carrier, a broad electrochemical spectrum, and physicochemical properties (Zhang
 93 et al., 2021; Reddy et al., 2022; Jia et al., 2022). As a result of its outstanding optical, thermal,
 94 electrical and mechanical properties as well as its high specific surface area, graphene has emerged
 95 a revolutionary material with wide range of applications, including its use as innovative adsorbents
 96 for water treatment (Igbal et al. 2020; Qu et al., 2022). It's an excellent adsorbent for removing a
 97 wide range of inorganic and organic pollutants because of its high surface area, abundance of
 98 active sites and excellent delocalized electron systems (Hossain et al., 2020). Despite significant
 99 progress made in the development and application of grapheme-based adsorbents, some inherent
 100 disadvantages remain.

101
 102 The hydrophobic nature of its surface and ease of aggregation in hydrous solution are
 103 disadvantages of graphene both of which significantly reduce its adsorption capacity in practical
 104 applications (Li et al. 2019). During liquid processing graphene even rolls to form graphite.
 105 Aggregation can limit its adsorptive application by blocking active sorption sites, decreasing
 106 theoretical surface area and impeding rapid mass transport (Phoon et al., 2020). Functionalized
 107 graphene can be designed to address some of these limitations. It is essential to understand the

108 adsorption efficiency of graphene-based materials and how it correlates to the mechanisms of
109 interaction between adsorbents and contaminants in order to advance the development of its
110 functionalized composites and their applications in waste treatment (Wang et al., 2021a). As a
111 result of their high surface area and abundance of active sites, there has been considerable interest
112 in graphene-based materials as potential adsorptive pollutants removal from water. The underlying
113 adsorption mechanisms are used for creating graphene-based adsorbents for target pollutants.
114 Reports on composite GO and semiconductor photocatalytic materials have increased in recent
115 years and GO as a good carrier for photocatalysts has improved the properties of materials
116 developed (Zhang et al. 2020; Liu et al. 2012). GO/Ag₃PO₄ composite material and the GO sheet
117 was coated with Ag₃PO₄ nanoparticles. In photocatalytic degradation experiments, composite
118 materials outperform pure Ag₃PO₄ in photocatalytic performance. This chapter discusses recent
119 advances in the graphene synthesis and graphene-based materials and its applications in
120 biomedical treatment via adsorption and photocatalytic methods. The present review begins with
121 the synthesis, adsorptive and photocatalytic treatment, isotherm and kinetic study, reusability and
122 mechanisms of graphene-based materials in biomedical waste treatment. This review is expected
123 to provide relevant existing knowledge and stimulate fresh ideas for the development of safe and
124 efficient graphene nanomaterials-based biomedical devices. With the development of graphene
125 nanoparticles, numerous other cutting-edge materials will also surely be found, and numerous
126 futuristic technologies will also become feasible.

127

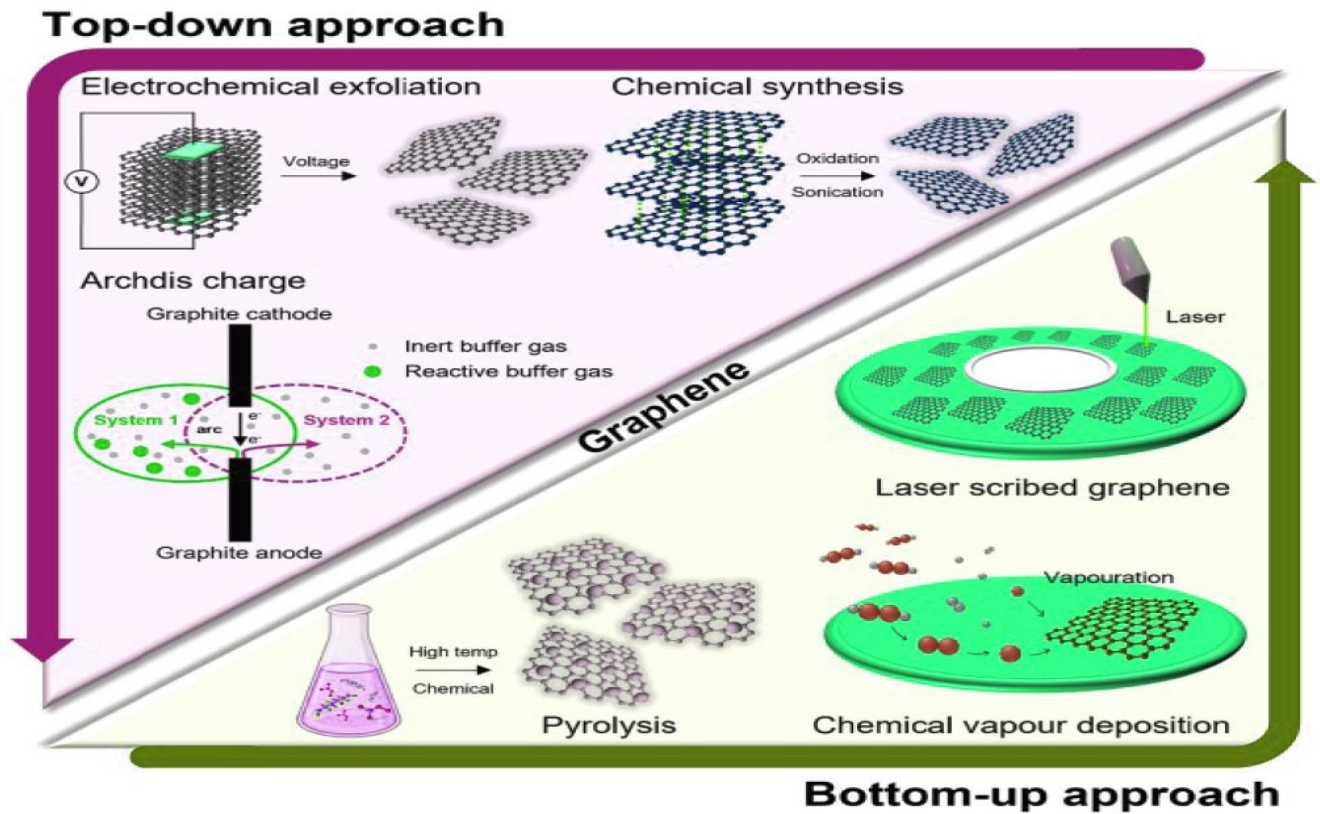
128 **2. Synthesis of graphene nanostructures**

129 The extraordinary electronic, surface, mechanical and optoelectronic attributes (properties) of 2-
130 dimensional graphene- a crystal lattice of carbon atoms are intriguing, making it possible to
131 develop various innovations across a broad spectrum of industries (Lim et al., 2018; Ikram et al.,
132 2020). The term "graphene synthesis" refers to any process, whether chemical or mechanical, that
133 is used to produce graphene with the desired level of purity and dimensions of the finished product
134 (Somasekaran et al., 2022). Currently, graphene synthesis processes can be classified into two
135 types namely; top-down and bottom-up (Kumar et al., 2021; Reddy et al., 2022). The graphical
136 illustration of the Top-down and Bottom-down synthesis approach is presented in Fig. 2.

137 2.1 Top-down approach

138 2.1.1 Mechanical exfoliation

139 A well-known and scientific way to mono-layered graphene-flakes extraction on preferred
140 substrates is mechanical exfoliation. It is formed when layered materials are subjected to transverse
141 or longitudinal stress (Yi and Shen, 2015; Ikram et al., 2020). Mechanical exfoliation is also
142 regarded as a low-cost method of synthesizing graphene. Graphene can be fabricated by stacking
143 single graphene carbon atoms using van der Waals forces with bonding energy and inter-spatial
144 values of 2 eV/nm² and 3.34Å respectively (Bhuyan et al., 2016). Mechanical cleaving, on the
145 other hand, involves an external force of about 3 μN/mm² for the separation of mono-atomic layer
146 from graphite. Sheet stacking is caused by a partially filled *p*-orbitals overlapping perpendicularly
147 on the sheet's plane with van der Waals forces inclusive (Zhang et al., 2005). Exfoliation is the
148 inverse of stacking and results in weak bond strength as well as wide vertical lattice spacing. It
149 does, however, results in bond improvement and tiny lattice spacing in the hexagonal lattice plane
150 (Gao et al., 2018). Several materials made from such as natural Gr (Lin et al. 2017), highly ordered
151 pyrolytic Gr (Zho et al. 2016). Graphene sheets Synthesis with different thicknesses alongside
152 mono-crystal Gr, have been observed as a result of mechanical exfoliation (Assouik et al., 2016).
153 The exfoliation method used scotch tape (Lin et al., 2013a), ultra-sonication (Compton et al.,
154 2012), transfer printing technique (Song et al., 2017), and electric field (Santos and Kaxiras, 2013).
155 Mechanical exfoliation has the disadvantage of producing a low yield of graphene



156 Fig.2. Graphical illustration of the Top-down and Bottom-down synthesis approach (Source:
 157 Reddy et al., 2022)
 158

159 2.1.2 Chemical reduction

160 Another top-down technique for producing graphene is chemical reduction of graphite-oxide.
 161 Graphite-oxide is always produced by oxidizing graphite. Oxidants like KMnO_4 , H_2SO_4 and nitric
 162 acid can be used to perform oxidation (Lim et al., 2018). GO reduction and sonication are also
 163 alternatives to graphene synthesis (Shin et al., 2009). Alkaline solution, ascorbic, hydrazine,
 164 glucose, hydroquinone, pyrrole, hydroxylamine, and phenyl hydrazine are some other reducing
 165 agents that can be used (Zhang et al. 2010; Stankovich et al., 2007; Wang et al. 2008; Zhou et al.
 166 2011). The hydrophilic nature of GO makes it a potentially useful material. In other to fabricate a
 167 mono-layered or double-layered GO, GO is first suspended in H_2O using sonication followed by
 168 surfaces deposition by filtering or spin coating (Iqbal et al., 2020). As a result, graphene films can
 169 be synthesized by thermally or chemically reducing GO. Furthermore, to create reduced GO
 170 dispersions in the non-polar solvents, a straightforward method like ‘solvo thermal reduction’ is
 171 advantageous. Although this process allows for mass production, it is difficult to produce a high-
 172 quality product due to the presence of some accompanying defects at the edges and deformation

173 (Paredes et al., 2011). Environmentally friendly approaches to limiting the utilization of hazardous
174 chemicals have grown in popularity in recent years (Aunkor et al., 2016). For instance, reducing
175 agents, such as ascorbic acid, have been used to create a benign synthesis process (Bo et al., 2014).
176 Electrochemical reduction is another method that can be utilized for large-scale graphene
177 synthesis. This procedure removes a huge number of oxygen functional groups while also
178 improving functional and electrical properties (Mohan et al., 2016). Thermal reduction of GO, in
179 addition to chemical and electrochemical reduction, is regarded as an efficient method for
180 producing high-performance rGO powders (Wu et al., 2011). The process (reduction) takes place
181 in an unreactive environment at a high heating rate. GO undergoes reduction by evaporating and
182 burning water molecules and oxygen functional groups at high temperatures (above or near 1000
183 °C). The pressure generated by the heating process determines the effectiveness of thermal
184 reduction (Tang et al. 2011).

185 2.1.3 Chemical exfoliation

186 Chemical exfoliation

187 Another efficient top-down method of graphene synthesis is chemical exfoliation. Chemical
188 exfoliation is divided into two steps. First, van der Waals forces reduction between the inter-layers
189 thereby increasing the Gr interlayer spacing. Second, a rapid heating process for Gr exfoliation
190 into single-layers and few-layers (Lim et al., 2018). The Brodie (Brodie, 1859), Staudenmaier
191 (Staudenmaier et al., 1898), and Hummers (Hummers and Offeman, 1958) techniques have been
192 used to create GOs. The Hummers method evolved, giving rise to modified and improved
193 Hummer's method (Chen et al., 2013). Table 1 compares the differences, types of oxidants used,
194 toxicity, and potential benefits of the different methods. The main benefit of Hummer's method is
195 scalable and low economic cost. The method is useful in producing large-scale graphene sheets,
196 making it suitable for industrial applications. Hummer's method is also a fast synthetic process,
197 which makes it ideal for mass production. The improved Hummers technique is preferred to make
198 graphene because it has low free toxicity and can make more organized graphene structures
199 (Obayomi et al., 2022).

200

201

202 Table 1. Chemical exfoliation methods for graphene synthesis: -overview

Method	Oxidants used	Toxicity	Advantage	Disadvantage	References
Brodie method	HNO ₃ & KClO ₃	Yes	-Laid principle for the delamination of Gr in G sheet by oxidation.	-Risk of explosion due to KClO ₃ usage. - Slow recovery progression - Product dispersibility in basic solution, small size, limited thickness, and imperfect structure	Brodie (1859); Botas et al. (2013)
Staudenmaier method	HNO ₃ , H ₂ SO ₄ , & KClO ₃	Yes	-Single step -Oxidation process. - Improved Process efficiency.	- Slow process. - Requires high operational temperature. - Bears risk of explosion. -Toxic	Staudenmaier (1898); Ikram et al. (2020)
Hummer's method	H ₂ SO ₄ NaNO ₃ & KMnO ₄	None (NO _x is released)	-Operates at low temperature. -The process is fast and efficient. -No Chances of explosion -Suitability for large scale GO production. -When compared to the Brodie and Staudenmaier methods, the oxidation level is higher. -Acid fog formation elimination. -Within hours, the reaction was completed.	-Incomplete oxidation. -Difficulties in removing of residual Na ⁺ and NO ₃ ⁻ ions from wastewater. -Purification and separation are both time-consuming processes. -Toxic gases are generated. -Low yield of product.	Hummers and Offeman (1958); Bota et al. (2013); Talyzin et al. (2017)
Modified Hummers method	H ₂ SO ₄ NaNO ₃ and KMnO ₄ or H ₂ SO ₄ and KMnO ₄	None (NO _x is released)	-Improved oxidation level enhances the GO performance. -Increased reaction yield. -Toxic gas emissions were reduced.	-Exhausting procedures for purification and separation are involved. - The process is time consuming.	Chen et al. (2013); Ikram et al. (2020)
Improved Hummers method	H ₂ SO ₄ , H ₃ PO ₄ and KMnO ₄	None	-More organized structured GO is produced. -The basal plane defect was minimal -The procedure is eco-friendly. -No toxic gases produced. - High GO yields. -The same level of conductivity results from same oxidation level.	-Purification and separation processes can be very laborious and lengthy.	Chen et al. (2013); Lim et al. (2018) Ikram et al. (2020)

203 (Source: Obayomi et al., 2022)

204

205 2.1.4 Liquid phase exfoliation.

206 Liquid phase exfoliation is a method widely used for graphene synthesis. This synthesis process is

207 broken down into three main phases: first, the graphene derivatives to be produced are dispersed

208 in a suitable solvent; next, the graphene is exfoliated; and finally, the derivatives of exfoliated
209 graphene are separated from their parent material during purification step (Niu et al., 2016). The
210 appropriateness of the solvent can be evaluated based on its "surface tension," "surface energy,"
211 and "Hildebrand and Hansen solubility," among other characteristics. As a result, graphene
212 dispersion can be achieved by making use of a wide range of aqueous and non-aqueous liquids
213 (Hernandez et al., 2008). Typically, for graphene exfoliation, the ideal surface tension is 0.4–0.5
214 J/m² and surface energy is 0.70–0.8 J/m² for the solvent. Because they have surface energies
215 similar to that of graphite, they have lower mixing enthalpy and thus a simpler process exfoliation
216 (Yi and Shen, 2015). Brodie began graphite production using solvent made from potassium
217 chlorate (KClO₃) and nitric acid (HNO₃) and oxidized graphite to produce GO. Staudenmaier
218 successfully extracted oxidized GO using the same solvent (Fang et al., 2009). Their method,
219 however, has become unpopular because of lengthy processing time and the use of potassium
220 chlorate which is hazardous. Hummers created GO in concentrated sulphuric acid (H₂SO₄),
221 potassium permanganate (KMnO₄) and sodium nitrate (NaNO₃) solvents (Hummers & Offeman,
222 1958). However, the GO produced through this method is more oxidized than previous methods
223 and the presence of non-oxidized graphite core in the GO necessitates a pre-treatment for the
224 improvement of the oxidation process (Kovtyukhova et al., 1999). Also, Hernandez et al. (2010)
225 investigated solvent's effect on graphene production using over 40 different solvents. An
226 extremely efficient method for producing graphene with minimal solvent was developed by the
227 researchers. Although liquid phase exfoliation is a common method of producing graphene,
228 sonication can cause some defects on the edge and basal planes (Iqbal et al., Amiria et al., 2018).
229 Sonication time is important because it affects graphene concentration. It was previously found
230 that the more prolong the duration of sonication, the greater the graphene concentration
231 (Hernandez et al., 2010). In graphene exfoliation, centrifugal force is also important. High
232 centrifugal force produces thinner graphene flakes (Ciesielski and Samori, 2014). The liquid
233 exfoliation process results in defects on graphene that can be reduced by adjusting the sonication
234 time, temperature, and intensity (Amiria et al., 2022).

235 236 2.1.5 Electrochemical exfoliation

237 Chemical or mechanical graphene synthesis has several processing limitations, including a time-
238 consuming and labor-intensive procedure, the use of hazardous and environmentally harsh
239 solvents/reagents and their regularity in quality as well. Though the processes for producing high-

240 quality graphene have been proposed, such as thermal decomposition of silicon carbide (SiC),
241 micromechanical cleavage and CVD, relatively low production rates and high costs, make them
242 they impractical for commercial applications. Electrochemical exfoliation proves to be a suitable
243 method for bulk synthesis of graphene in less time and at minimal cost. It is safer because no harsh
244 chemicals are used in this process. It is a method of using an electrical current to exfoliate a
245 graphite electrode in a liquid electrolyte. In this process, the working electrode is usually a graphite
246 film/rod /highly oriented pyrolytic graphite sample. Another counter electrode made of the same
247 graphite/nickel/iron/platinum alloy could be used. Migration of ions (+ve charged) from the
248 electrolyte to the working electrodes is caused by a potential difference created between two
249 electrodes, and become interposed among the graphene layers of graphite. This process known as
250 intercalation produces the impetus to disband the van der Waals forces, resulting in the expansion
251 of graphite structurally. The graphite electrodes properties such as particulate size, layer
252 arrangements, defects, thickness and appropriate pre-treatment, is also expected to influence ion
253 intercalations (Aghamohammadi et al., 2020; Nayak et al., 2022)

254 255 2.2 Bottom-up-approach

256 2.2.1 Epitaxial growth on silicon

257 Epitaxial growth is known as the growth layer of a substance on a substrate that continues the
258 crystal structure of the substrate. There is tendency for silicon carbide wafer to sublime when
259 subjected to specific conditions: high temperatures at 800 to 1150 °C and vacuum conditions at
260 109 to 1010 mbar or at 1500 °C under noble argon gas. Hence, leaving the carbon remaining on
261 the substrate to form graphitic layers on the wafer's carbon or silicon faces (Kumari, 2021). As one
262 might expect, silicon carbide to have a lattice structure similar to graphene. Unlike chemical
263 vapour deposition (CVD), epitaxial growth enables the production of large surface-area graphene
264 sheets. This is a transfer-free process that is dependent on the substrate's crystallographic
265 orientation, meaning that transferring the graphene requires no peculiar technique. The mechanism
266 of graphene epitaxial growth consists of two steps: nucleation and layer-by-layer growth (Yazdi
267 et al., 2016). Based on the substrate, there are types of epitaxial growth processes: homo-epitaxial
268 growth and hetero-epitaxial growth. Homo epitaxial growth process normally involves film
269 deposition on same material as the substrate. When the film and substrate are made of different
270 materials, a hetero-epitaxial structure is formed. Silicon carbide was first applied for measuring

271 electrically on patterned epitaxial layers (Ikram et al., 2020). Edward Goodrich Acheson invented
272 this process in 1893, when he devised a technique for synthesizing silicon carbide (SiC) by heating
273 various carbonaceous sources. At temperature greater than 4000 °C, the author discovered that
274 pure crystalline graphite was formed (Acheson, 1896; Iqbal et al., 2020). As far as large-scale
275 production is concerned, this method looks promising. The epitaxial growth method, on the other
276 hand, has a very high production cost due to its intensive energy features and the prohibitively
277 high cost of single crystal commercially available silicon carbide substrates (Choi et al., 2010).
278 Another significant limitation of this method is non-uniformity. Furthermore, Si-face graphene is
279 preferred over C-face graphene because it has better graphene growth uniformity. Until now, this
280 method has been underutilized due to a lack of knowledge about the growth and interaction
281 mechanisms of graphene and the SiC substrate (Li et al., 2009).

282 283 2.2.2 Chemical vapour deposition on metal catalyst

284 CVD is a straightforward method which utilizes carbon precursors in its gaseous state e.g.,
285 methane to produce graphene. High surface area, single-layered and few-layered graphene can be
286 grown on copper substrates (Lim et al., 2018). This method can produce high surface areas of
287 monolayer graphene (a few cm²). CVD has the potential to develop into a technology that is viable
288 for commercial use. The solubility of carbon in metals is the fundamental premise behind the CVD
289 process. Hydrocarbons and other gaseous carbon precursors are introduced into a reactor that is
290 able to withstand high temperatures. Once inside, the hydrocarbons and other gaseous carbon
291 precursors break down and dissolve into metal substrates (Alshamkhani et al., 2021). The
292 difference in carbon solubility at different temperatures causes carbon to precipitate out of solid
293 carbon-metal solutions. The growth substrate in the CVD process is the most significant aspect in
294 the formation of graphene which starts from hydrocarbon decomposition and succeeded by
295 evolution of metal substrate with carbon atom deposit (Kumari, 2021). It is difficult to transfer
296 graphene to a substrate of interest from the growth substrate because graphene has a low chemical
297 response. As a result, the fabric begins to show flaws and wrinkles (Kumar et al., 2021). In
298 addition, the procedure is complicated and energy-intensive, which restricts the task at times. The
299 CVD process, however, remains the most auspicious high surface-area graphene production
300 technique. In the CVD process, graphene is deposited on different of metal plates (substrates),
301 including Cu, Ni, Ir, Pd, and Ru (Reina et al., 2009; Kim et al., 2009; Coraux et al., 2008; Choucair

302 et al., 2009). Copper and nickel are the most commonly used substrates for CVD growth of
303 graphene (Bouhafs et al., 2021).

304

305

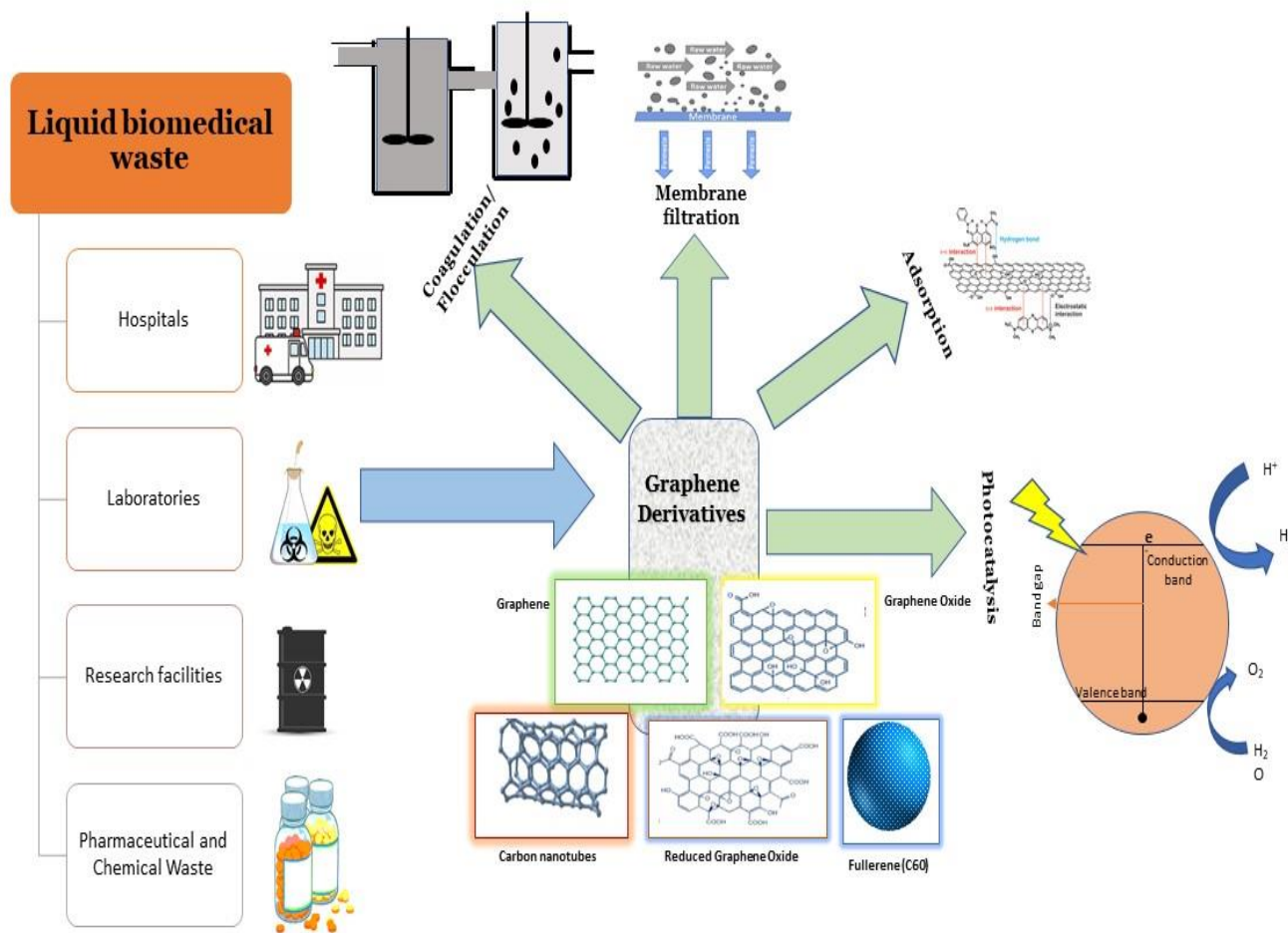
306 2.2.3 Organic synthesis

307 Polycyclic hydrocarbons (PAHs) can be used to create graphene, specifically graphene
308 nanoribbons (GNRs). Unlike the CVD method, which produces GNRs with widths of 30–200 nm,
309 GNRs with widths of less than 10 nm can be produced by organic synthesis, making it easier to
310 engineer their band-gaps. Nevertheless, Gr synthesis from polycyclic hydrocarbons is tough
311 because C–C bonds formation is required in a single step as well as the activation of inert C–H
312 bonds in polycyclic hydrocarbons enabling those bonds to participate in the reaction. This makes
313 the process time-consuming and complicated. Notwithstanding, there have been developments in
314 chemical processes that are both quick and efficient (Basagni et al., 2015) with many of them
315 predicated on oxidative cyclodehydrogenation (Scholl reaction) (Salvatierra et al., 2015). Diels-
316 Alder polymerization, cyclotrimerization, and photocyclization are other methods for organic
317 graphene synthesis (Zhang et al., 2010; Liu et al., 2014). These techniques are not only
318 necessitated, there is limitation in the number of products produced.

319 3. Biomedical waste treatment using graphene

320 As the world's population expands so is medicines and healthcare products demand to treat
321 diseases. Thus, there is a need to channel resources and technology towards improving and
322 promoting the manufacturing of various pharmaceutical and medical products. However, the lack
323 of proper techniques and the use of sub-optimal approaches to waste minimization during
324 production, post-production and/or treatment stages by pharmaceutical industries or health care
325 facilities generate effluents that are released into the environment untreated (Patel et al., 2022).
326 Sustainable and safe management of biomedical waste is a global challenge because of its potential
327 hazard to human the environment and health. The increased generation of biomedical wastes from
328 various health care facilities, including hospitals, clinics, and nursing homes, has also become a
329 matter of concern in many countries. Removal of toxic metal ions, recalcitrant organic pollutants,
330 and pharmaceuticals by various emerging technologies has been the primary focus of research over
331 the course of the past decade (Majumder et al., 2021). Treatment of biomedical waste can be
332 accomplished in various ways including through the application of physical, chemical, and

333 biological processes. It is important to consider the type and quantity of waste to be treated when
 334 deciding about which of these technologies to employ. Nevertheless, the majority of these
 335 techniques including advanced oxidation processes, electrochemical purification, membranes
 336 processes, and many more are not eco-friendly and may pose health risks to both employees and
 337 the general public as well. Nonetheless, adsorption and photocatalytic methods seems to overcome
 338 these challenges which make it more preferred as it outperforms other techniques due to its ease
 339 of operation, cost-effectiveness, flexibility, technological feasibility, absence of byproducts, and
 340 the ability to be easily recycled. (Cao et al., 2021). The various methods for treatment of
 341 biomedical waste using graphene and its derivatives is presented in Fig. 3.



343 Fig. 3: The various methods for biomedical liquid waste treatment using graphene and its
 344 derivatives

345
 346 3.1 Infectious biowaste treatment

347 Generally, biomedical waste tends to be cytotoxic, injurious, chemical or infectious. Infectious
348 biomedical waste contains substances which have deleterious effects on biological organisms.
349 Biomedical waste is hazardous since it has the potential to spread infections. Once the waste
350 becomes contaminated with biohazardous agents, they pose the risk of disease transmission. They
351 include waste from lab cultures, isolation wards, equipment that have come in contact with infected
352 patients, infected clinical specimens, tissue from experimental animals, cotton swabs and excreta
353 as well as soiled mattresses and beddings from blood or body fluids (Reddy et al., 2014). Hospital
354 wastewater is a major breeding ground for antibiotic-resistant bacteria, making it a potential vector
355 for human and environmental infection (Amine, 2013; Shahzad et al., 2021). The importance of
356 managing biomedical waste is critical, particularly in medical facilities. This is due to the fact that
357 improper segregation, biomedical wastes disposal, and inclusion of biomedical waste in municipal
358 waste making healthcare workers and the general public vulnerable (Makajic-Nikolic et al., 2019).
359 Hence, infectious biomedical waste management should be a top priority for hospitals and other
360 medical facilities. Although it is common knowledge that efficient wastewater treatment
361 technologies are required to harness the control of infectious waterborne pathogens, it is
362 unfortunate that the present options available for managing biomedical waste do not address the
363 current danger that is posed by liquid effluent discharges, which is a significant issue for healthcare
364 facilities. GO, a function form of graphene with excellent electrochemical properties and
365 functional groups e.g. -COH, -OH, and R-O-R can be applied in wastewater treatment. Although
366 no studies have been reported in literature on the utilization of graphene as an adsorbent for the
367 treatment of infectious biowaste and therefore we proposed that this area of research will be viable
368 and require attention. In environmental fields, attention has been drawn to the use of nanoparticles
369 due to the rapid development of nanotechnology. Effective microbial decontamination and
370 pathogen disinfection is critical to controlling transmission and thereby reducing risk of infection
371 (Rikta, 2021).

372 Reduced GO possesses antimicrobial properties, which hinders bacterial growth and therefore the
373 biofilm formation on the filter surfaces (Hu et al., 2010). Physical and chemical properties such as
374 stability, reactivity and large surface area makes nanoparticles outstanding and also preferred
375 catalysts and adsorbents (Li et al., 2008; Rikta and Tareq, 2017; Rikta, 2016).

376 Bao et al., (2011) impregnated GO nanosheets with silver nanoparticles and applied them for
377 microbial disinfection and found them effective for inactivating *Escherichia coli* and
378 *Staphylococcus aureus* with 100% and 87.6 % removal efficiency.

379 Gollavelli et al. (2013) utilized smart magnetic graphene resulting from graphene oxide and
380 ferrocene precursors to inactivate *Escherichia coli* with 100 % removal efficiency. Researchers
381 have also suggested possible mechanisms responsible for the destruction and inactivation of
382 microorganisms including- Production of toxic reactive oxygen species (ROS) due to the GO's
383 interaction with wastewater through the cell protein and genetical material damages (Rikta et al,
384 2019), microbial disinfection is achieved via the Sharp edges present in graphene and GO which
385 aid microorganisms' destruction physically (Smith and Rodrigues, 2015). Additionally, various
386 research has proposed obstruction to nutrients diffusion into microbial cells by graphene sheets
387 causing cell wrapping leading to the suppression in the growth of micro-organisms (Liu et al.,
388 2011; Chen et al., 2014).

389 3.2 Hazardous biowaste treatment

390 Hazardous wastes are generated from industries, hospitals some household wastes. Hazardous
391 waste is defined by the United State Resource Conservation and Recovery Act (RCRA) as a of
392 solid-liquid wastes combination that may give rise to or contribute substantially to an increase in
393 morbidity due to their concentration, quantity, or physical, chemical, or infectious characteristics.
394 According to the EPA, hazardous wastes “possess properties which make them dangerous or
395 capable of having a harmful effect on human health or the environment”. Large amounts of
396 hazardous substance-containing effluent are discharged into the environment resulting from
397 industrialization and urban development processes (Wiśniewska et al., 2017). They can increase
398 the risk of motility because they are corrosive, flammable, or have a high affinity and readily react
399 when exposed to other substances (Letcher and Slack, 2019; Muralikrishna and Manickam, 2017).
400 Toxicity is the most concerning of these characteristics due to its impact on human beings and
401 other living organisms. Hazardous pollutants sources include hormones, pesticides, antimicrobial
402 agents, illicit drugs, pharmaceuticals and personal care products (Margot et al., 2015). The waste
403 generated during the production of pharmaceuticals varies greatly in amount and type and is
404 relatively more than the actual finished product. The term "pharmaceutical wastewater" primarily
405 refers to effluents and wastes generated during pharmaceutical manufacturing. There can be
406 anywhere from 200 to 30,000 kg of waste produced for each kilogram of active ingredient

407 produced (NRDC 2009; Lefebvre et al., 2014). The amount of wastewater produced by
408 pharmaceutical manufacturing facilities grows as the industry expands. The current rate of
409 improper disposal of unused medicines from hospitals and households is concerning (Santos et al.,
410 2007, Tong et al., 2011, Vellinga et al., 2014). Pharmaceutical waste is broadly classified as: a)
411 waste generated by pharmaceutical companies and effluents from treatment and recycling plants
412 handling such wastes, and medical waste from hospitals and households, which significantly
413 contaminates sewage systems. The latter is to blame for the presence of pharmaceutically active
414 compounds (PhACs) in public sewers and, as a result, municipal wastewater treatment plants
415 (Baumgarten et al., 2007; Pal, 2018). Analgesics, broncho spasmolytics, antibiotics, cosmetics,
416 contraceptives, anti-depressive agents, non-steroid anti-inflammatory drugs (NSAIDs), lipid
417 regulators, antiseptics, anti-rheumatic beta blockers, and diuretics have been discovered in the feed
418 of municipal wastewater treatment plants as well as in the effluents of sewage-treatment plants to
419 a scale of g/ml (Ahmed et al., 2017; Pal, 2018). Various treatment options are available for treating
420 pharmaceutical wastewater, but due to the complex nature of the effluents, treatment can be
421 challenging.

422 Gadipelly et al., (2014) and Zaied, et al., (2020) in their studies gave a comprehensive list of
423 composition of the wastewater generated in pharmaceutical industries and active ingredients.
424 Various treatment technologies exist and have been adopted for treatment of pharmaceutical
425 wastewater as presented in Table 2. As a result of the complexities of industrial effluents, there is
426 no one-size-fits-all method, and currently, no single method capable of adequate treatment is
427 available. For example, despite the success of anaerobic digestion technologies in treating high-
428 strength antibiotic wastewater with benefits such as biogas production and reduced waste sludge
429 production (Ma et al., 2018), issues such as long start-up times, slow anaerobic microorganism
430 growth rates, and poor biomass retention persist (Huang et al., 2018).

431 The investigation of the adsorption efficiency by Gao et al., (2012) of tetracycline by GO reveals
432 that the removal of tetracycline is achieved majorly through a π - π and cation- π interactions with a
433 maximum monolayer adsorption capability is 313 mg/g and it decreases with increase in the
434 solution's pH or the sodium ions concentration. Moreira et al. (2020) demonstrated the
435 simultaneous adsorption and degradation of norfloxacin (NOR) in an aqueous matrix by GO. The
436 authors reported that the 8 layers GO was created through oxidation or exfoliation of the enlarged
437 graphite using a modified Hummer's method. The removal capacity of the GO adsorbent was 374.9

438 ± 29.8 mg/g, with higher input from the NO-R in the zwitterionic form and removes about 94.8 %.
439 The intra-particle diffusion process, as measured by Boyd's model and Fick's law, contributed
440 more to the removal process and reaches equilibrium half hour after it began. Finally, the process
441 underwent scale up in a single-stage batch adsorber with a 95% efficiency of NOR removal.

442 Rajabi et al. (2019) also reported the treatment of hazardous chemical and strong mutagen ethidium
443 monoazide bromide (EMA) from aqueous solution using a GO adsorbent surface. The authors also
444 reported on the investigation of variables such as solution temperature, contact time, ethidium
445 monoazide bromide initial concentration, and pH affecting the process. EMA adsorption result on
446 GO, the optimum time and pH, respectively, were 17 min and pH 10. The authors reported its
447 maximum adsorptive efficiency of 76.92 mg/g at 303 K.

448 **Table 2: Pharmaceutical waste treatment**

Treatment technology	Examples	Type	Sub type	Operation	Merits	Demerits	References
Biological treatment	PPCPs and Endocrine disruptors	Vermicomposting		Use of earthworms to convert organic materials (usually waste) into a humus-like material	Pharmaceutical wastes are broken down and converted to harmless or useful forms		Innemanová et al., (2022)
		Composting		sludge mixed with carbonaceous matter (e.g., sawdust, wood chips)	Reduce secondary pollution and treatment of sewage		Haiba, et al., (2013)
		anaerobic treatment			biogas production, less waste sludge production and cost effectiveness	Default start-up time is lengthy, slow-growth rates of anaerobic microorganisms	
		activated sludge	Biological reactor	Membrane bioreactor Sequencing bioreactor	high volume load and fast reaction speed produce high quality effluent devoid of suspended solids		
Physicochemical method	oxytetracycline, gentamicin and tetracycline	coagulation-flocculation		Agglomeration, uptake of pollutants and separation of products formed	Biodegradation performance of the wastewater is greatly enhanced. Reduction in the concentration of the pollutants	generation of secondary waste	
	doxycycline	Electrocoagulation			Efficient elimination of SS, oils, greases, color and metals	Flocs will need to be filtered, requires post treatment	
	PPCPs (100%)	membrane technology	membrane filtration	Nondestructive separation	Small space requirement, high	High operational cost, rapid	Wang, et al., (2018)

			efficiency even at high concentrations, no chemicals are used	membrane clogging
		microfiltration/ultrafiltration/nanofiltration		
		Reverse osmosis		
Adsorption		Surface chemistry and pore-size distribution	It allows for easy elimination of most micropollutants whilst averting byproducts formation.	Recycling and management of spent adsorbent waste Initial cost of the selective resin, the acidity level in the water can be increased to allow sodium ions to enter the softened water, making the water unsafe to use.
ion-exchange			No perforation of substances into the soft water	
chemical reduction				
Constructed wetlands			High removal efficiency of micropollutants from pharmaceutical wastewater, cost effective and low energy usage	

Advanced Oxidation Processes	Cetirizine	electrochemical processes	Electro-oxidation	Oxidizing agents	Good processing efficiency, easy to operate, and offers recyclability of useful materials,	Using AOPs solely to handle large amounts of wastewater is not cost-effective.	Agnihotri et al. (2018)
	sulfamethazine	Fenton process	Electro-chemical reduction		Organic matter is easily targeted and oxidized.	The technology is not mature for full scale and industrial use	Tang and Wang (2018)
			Electro-fenton	Reactive species (OH ⁻ , SO ₄ ²⁻)			
	tetracycline hydrochloride	Photocatalysis	Fenton like	Photo-fenton		remove harmful organic substances in wastewater	
N,N-dimethylacetamide	Ozonation//catalytic ozonation				increase the biodegradability of the pharmaceutical wastewater, Organic contaminants can be removed, disinfection and sterilization	Oxidative by-products are formed, Expensive to deploy	Peng, Yan, et al. (2018)

449

450

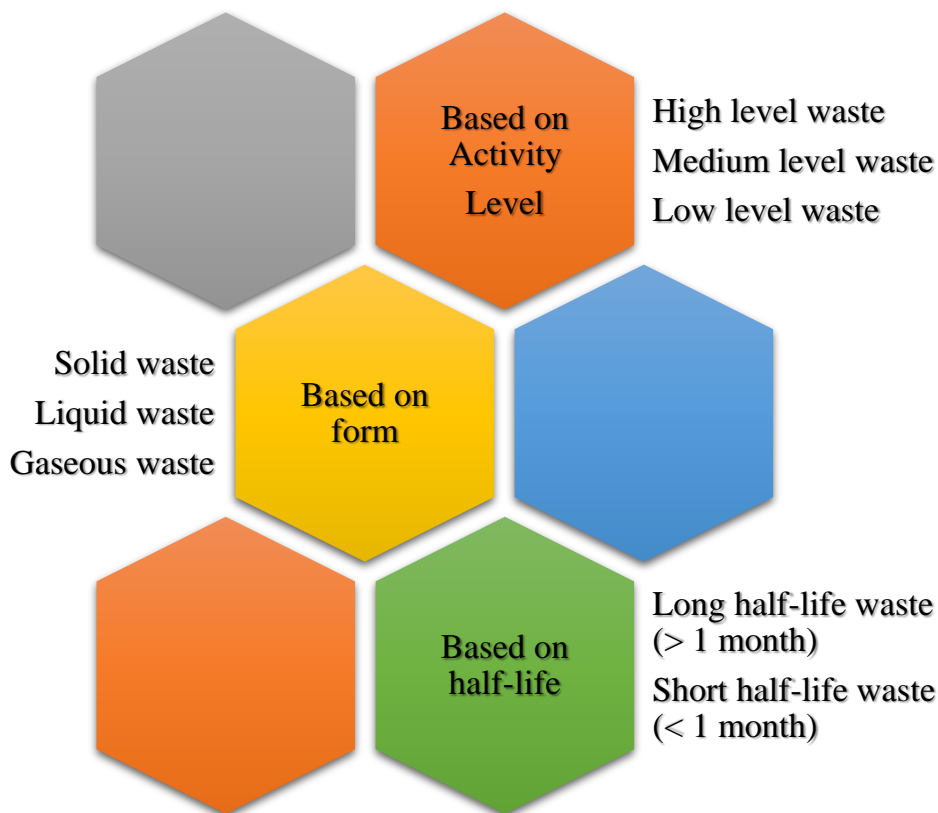
451

452

453

454 3.3 Radioactive Biowaste Treatment

455 Radionuclide application in medicine is a well-established field. When utilized appropriately in a
456 variety of medical applications for diagnostic, therapeutic, and research purposes, radioactive
457 materials have been found to be extremely effective (IAEA, 2000). Their usefulness, market
458 availability and reasonable price also make radioactive substances desirable. Handling these
459 materials has invariably led to the generation of biomedical radioactive waste in form of residues
460 and by-products. The amount and type of waste produced differ according to the size of the medical
461 application and the radionuclides used. Classification of radioactive waste can be made depending
462 on various attributes as shown in Fig. 4.



463

464 Fig.4. Various classifications of radioactive waste

465 With the exception of some medium-level waste, the majority of hospital radioactive waste is low-
466 level waste (low energy and emitters) with short half-lives. The nuclear industry and nuclear
467 reactors are typically associated with high-level waste (Khan et al., 2010). Different types of
468 radionuclides are utilized in hospitals and medical centers for “in vivo” and “in vitro” applications.
469 They have been implemented for diagnostics, research, and therapeutic uses. Radioactive waste

470 could be generated as solid or liquid wastes from radionuclide medical applications (Chartier,
471 2014). The major sources of liquid radioactive waste can be seen in Fig. 5. The radioactive waste
472 management plan must be exhaustive and take into account all facets, from radionuclide
473 procurement to the final release of waste packages from the facility for disposal/discharge. A good
474 management plan should consider both original and secondary waste sources, the latter being from
475 subsequent treatment and conditioning of the original. In any case that waste generation can be
476 avoided or at least minimized, it should be implemented as the most preferable option. When waste
477 prevention cannot be implemented, other approaches have been adopted. For instance, in some
478 countries, diluting the overall radionuclide content of waste is permitted under certain conditions.
479 Non-radioactive wastes are used to dilute low level radioactive waste in order to meet the
480 regulatory specifications (IAEA, 2000).

481

482

483

484

485

486

487

488

489

490

491

492

493

494

495

496

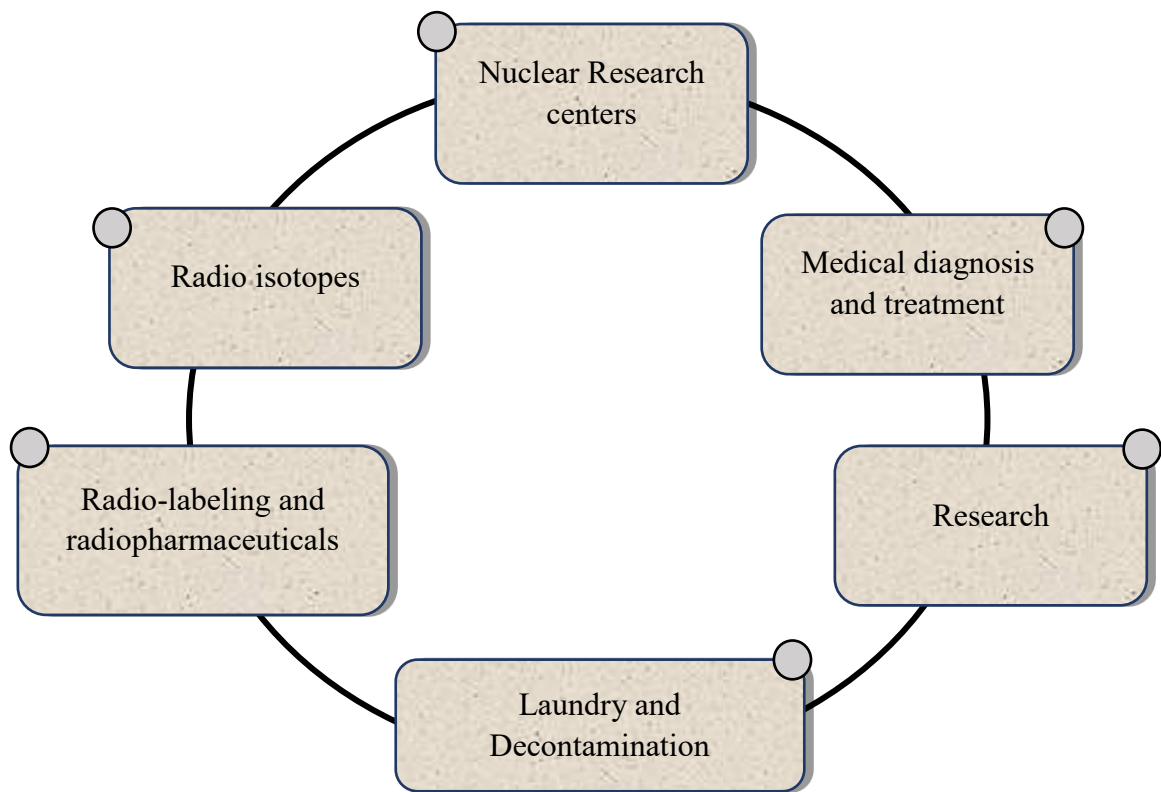


Fig.5. Sources of radioactive wastes

497 In order to ensure safe discharge into the environment, liquid radioactive waste must meet
498 extremely stringent requirements concerning radioactive substance limits and other impurities.
499 The treatment of liquid radioactive waste frequently involves the application of several steps such

500 as filtration, precipitation, sorption, chemical precipitation, sedimentation, flocculation, ion
501 exchange (Figueiredo et al., 2018), evaporation, and/or membrane separation to meet the
502 requirements for both the release of decontaminated effluents into the environment and the
503 conditioning of waste concentrates for disposal (Zakrzewska-Trznadel, 2013; Lehto, 2019). Ren
504 et al., (2008) performed experimental treatment on saline low-level radioactive waste containing
505 plutonium (^{94}Pu) and Uranium (^{235}U). Flocculation was used for successful removal of ^{94}Pu and
506 ^{235}U respectively under alkaline acidic conditions. A 95.5 % removal efficiency of ^{235}U was
507 observed. Dulama et al., (2008) used membrane technology combined with inorganic sorbents for
508 the treatment of radioactive liquid waste containing Cesium (^{137}Cs). The study found that using
509 natural zeolite in the pre-treatment stage resulted in greater ^{137}Cs removal efficiencies, which were
510 credited to the affinity of the materials for ^{137}Cs . Subsequently, various materials including
511 Inorganic adsorbents have been successfully employed to mitigate radioactive waste as an
512 alternative treatment technology. They possess high exchange capacity, possible selectivity, and
513 specificity, and are resistant to radioactive radiation. Emerging processes bearing higher efficiency
514 in recent times have been used in radioactive decontamination. Membrane technologies,
515 particularly pressure-driven ones such as reverse osmosis, microfiltration, and ultrafiltration, play
516 a large role in these processes. Membrane technologies outperform traditional processes in several
517 ways, including lower energy consumption, no chemical addition, operation at low temperatures,
518 and ease of scaling-up. Furthermore, a suitable combination of different processes can
519 simultaneously remove radioactive, organic, and biological substances. These processes have been
520 used successfully in the treatment of a variety radioactive effluents. Fouling, on the other hand, is
521 a major issue in membrane processes and can be caused by inorganic, organic, or even biological
522 substances. Membrane fouling reduces the flux that passes through the membrane, degrades
523 permeate quality, reduces membrane life and raises operating costs. Membrane fouling can be
524 reduced by using appropriate pretreatment operating parameters including composite membranes
525 matrices by the inclusion of TiO_2 , ZnO and graphene oxide nanomaterials with benefits such as
526 thermal, physical and chemical stability. Other alternatives such as graphene oxide and mixed
527 matrix membranes provide higher biofouling resistance, long-term stability and possible
528 regeneration of membrane material.

529

530 4. Graphene-based nanocomposites

531 The performance of graphene adsorbents is mostly determined by their uniform dispersion in
532 solution as well as their high sorption capacity to a variety of contaminants. Graphene often has a
533 high affinity to aggregate or even roll to form graphite during liquid processing (Hosseini, H., et
534 al., 2022). Aggregation can limit its adsorptive applicability by obstructing active sorption sites,
535 limiting theoretical surface area, and impeding rapid mass transfer. Due to the electrostatic
536 repulsion between them, GO has a low binding affinity to anionic dyes. Furthermore, due to its
537 high solubility, GO cannot be regenerated easily from wastewater treatment, resulting in secondary
538 pollution to the environment; hence, its application in pollutant treatment is limited (Chen et al.,
539 2021). All of these aforementioned drawbacks can be overcome by functionalizing GO with
540 various covalent or non-covalent dissimilar molecules, polymers, and nanoparticles, resulting in
541 the development of composites, a class of multicomponent materials (Ali et al., 2021). The
542 composite that results is more than just the sum of the separate components; it is a new substance
543 with new functionalities and qualities. (Nagarajan et al., 2022). The synthesis method and surface
544 area of various graphene-based nanocomposites reported from recent works is presented in Table
545 3 summarizes the recent works in the development of graphene composites materials. As a result
546 of their enormous surface area, enhanced stability avoiding π - π stacking between, and numerous
547 active sites for adsorption, graphene-based materials have attracted a lot of interest as appealing
548 candidate for adsorptive removal of contaminants from water. (Yan and Li, 2022). The underlying
549 adsorption principles are used to design graphene-based adsorbents for target pollutants. Better
550 understanding of graphene-based adsorption performance and how it relates to the interactions
551 between pollutants and adsorbents is crucial for the future development of graphene-based
552 functional materials and their practical applications. (Mahmoodi et al., 2019). Nagarajan et al.,
553 (2022) reported the fabrication of magnesium nanocomposites decorated with multilayer graphene
554 (MG) and its application in pollutant treatment in a recent study. The BET surface area of the
555 developed graphene-based nanocomposite was found to be 1480 m²/g. The synthesis of
556 Polypyrrole functionalized Cobalt oxide Graphene (COPYGO) nanocomposite via hydrothermal
557 method was explored by Anuma et al., (2021). The authors reported the BET surface area of 133
558 m²/g. Verma et al., (2022) functionalized graphene oxide-chitosan with EDTA for inorganic and
559 organic pollutants treatment. The BET surface area of 1.326 m²/g was reported by the authors. The
560 fabrication of graphene hydrogel decorated on nickel with BET surface area of 67.84 m²/g was

561 explored by Ebratkhahan et al., (2022). Chen et al., (2021) also reported the BET surface area
 562 41.54 m²/g for the fabrication of carbon layer encapsulated Fe₃O₄ /graphene oxide nanocomposites
 563 rich in amino and thiol groups (Fe₃O₄ @C /GO).

564 Table 3. Graphene-based nanocomposites synthesis and their respective surface areas

Graphene-based nanocomposite	Preparation method	BET surface area (m ² /g)	References
MG	Simple combustion process	1480	Nagarajan et al., (2022)
COPYGO	Hydrothermal	133	Anuma et al., (2021)
GO-EDTA-CS	modified covalent binding and electrostatic interaction process	1.326	Verma et al., (2022)
GH-Ni	polyol and hydrothermal	67.84	Ebratkhahan et al., (2022)
Fe ₃ O ₄ @C /GO	Solvothermal	41.54	Chen et al., (2021)
Gr ₅ -SBA/TiO ₂ NCs	co-condensation hydrothermal	340.45	Ali et al., (2021)
ZIF-8/CoFe ₂ O ₄ /GO	Ultrasound-assisted	2490	Mahmoodi et al., (2019)
Fe ₃ O ₄ /porous graphene nanocomposites.	Hydrothermal	410	Bharath et al., (2017)
CMC-PAA-GO	Freeze-drying	42	Hosseini et al., (2022)
Fe ₃ O ₄ /G-AC	catalytic <u>graphitization</u>	485.8	

565
566

567 5. Biomedical treatment using graphene-based nanocomposites

568 Graphene is fundamentally a monatomic graphite layer, a mineral-rich allotrope of carbon made
 569 up of tightly bonded carbon atoms organized in a hexagonal lattice. As a result of its sp²
 570 hybridization and extremely thin atomic thickness of 0.345 nm, graphene is a very distinct material
 571 (Reddy et al., 2019). However, its hydrophobic nature which makes it insoluble in hydrophilic
 572 solvents like water limits its application in water purification. In order to overcome this limitation,
 573 the hydrophobic nature must be compromised. To improve its affinity to aqueous solution,
 574 graphene's have been modified by adding functional groups on its surface through chemical
 575 modification, covalent, or noncovalent functionalization giving rise to the graphene-based
 576 nanomaterials. Owing to their attractive properties which include water-solubility, low toxicity,
 577 very good water dispersibility, antibacterial activity, high adsorption rate, graphene-based
 578 nanomaterials have more advantages over other materials such as high adsorption rate, high
 579 dispersion rate and antibacterial activity which makes them a better choice for biomedical

580 wastewater treatment (Balasubramani et al., 2020). Recently, graphene-based materials have
581 received a lot of attention as potential adsorbents for wastewater treatment. In wastewater
582 treatment, graphene is an intriguing carbon material having distinct advantages over other
583 adsorbents such as activated carbon, carbon nanotubes, chitosan, clay, and zeolite. Graphene is an
584 appealing material for use in wastewater treatment considering its increased surface area for
585 adsorption of biomedical contaminant species, as well as the possible chemical modifications and
586 composite fabrication (Yu et al., 2016; Jeyaseelan et al., 2021). As earlier stated, the modifiable
587 chemical properties of graphene alongside its large surface area, highly delocalized π -electrons
588 positions them as very captivating and auspicious for usage to adsorb pollutants in wastewater and
589 address environmental sustainability concerns. However, vehement inter-planar interactions make
590 graphene nano-layers jointly incline and also recombine to produce graphite. As a result of tough
591 electrostatic repulsion between graphene oxide and negatively charged compounds, the binding
592 affinity between them is weak.

593
594 Notwithstanding, the possibility of graphene alongside graphene oxide not composing and coming
595 off decontaminated effluents leads to serious re-contamination. Overcoming these disadvantages
596 is possible by functionalizing covalently or non-covalently using different molecules and other
597 nanoparticles, through which, nanocomposites - multi-component material groups are produced,
598 where one phase is dispersed into another in the nanometric range (Ali, 2019). Several researchers
599 have shown the high adsorption capacity of graphene-based materials and most studies consider
600 solution pH, ionic strength, and temperature as essential parameters in biomedical pollutants
601 treatment, in addition to the adsorbent's intrinsic properties (Ersan et al., 2017). Adsorption
602 interactions are non-covalent interactions that occur between pollutants and graphene-based
603 materials as presented in Fig. 6. However, the true nature of such interactions such as electrostatic,
604 hydrogen bonds, hydrophobic and Van der Waals interactions as well as their relative
605 contributions, are hotly debated (Kern et al., 2022). Their surface chemistry heavily influences the
606 adsorption and photocatalytic properties of graphene-based materials. Oxygen-containing
607 functional groups on the surface of GO have two opposing effects on adsorption capacity.
608 Adsorption can be boosted by increasing the water solubility on the surface of a surface charge;
609 however, there is a reduction in adsorption sites by the water clusters produced on the surface. The
610 oxygen concentration of graphene oxide, on the other hand, increases the adsorption of

611 contaminants such as amino acids and hydroxyl groups via strong hydrogen or Lewis' interactions
612 (Priyadharshini et al., 2022).

613
614 Gao et al., (2012) developed the GO as a potential adsorbent for the removal of Significant
615 concerns tetracycline antibiotics from aqueous environment. The authors observed that the
616 tetracycline was deposited strongly via π - π interaction and cation- π bonding on the surface GO.
617 The adsorption equilibrium data was found to fits well the Langmuir and Temkin isotherm model
618 with theoretical maximum of adsorption capacity 313 mg/g. The adsorption kinetics was well
619 described by pseudo-second-order model.

620 Komal et al., (2022) conducted an extensive study to evaluate the effect of percentage load of
621 functionalized graphene oxide on the development of various forms of modified GO supported
622 with functionalized cellulose nanofibers (CNF) obtained from excess biomass for the treatment of
623 toxic drug species from aqueous environments. The authors assessed the adsorptive performance
624 of the developed nanohybrids for the treatment of ciprofloxacin and ofloxacin and optimized their
625 performance varying adsorbent loading, pH, and initial drug concentration. Furthermore, different
626 kinetic and isotherm adsorption models were studied to investigate adsorbent properties and the
627 adsorption process. The adsorptive capability of functionalized CNF was significantly improved
628 by its easy aggregation with functionalized graphene oxide. The results of the experiments
629 revealed that a 20 wt% loading of carboxylated GO within the perforated surface of esterified
630 CNFs showed excellent adsorption efficiency, with peak at 45.04 mg/g for ciprofloxacin and 85.30
631 mg/g for ofloxacin uptake. The interaction of electronegative functional groups and deficient
632 structure found on CIP with aromatic structure found within GO basal planes and functionalized
633 GO edges can explain the underlying chemisorption mechanism. Hydrogen bonding is also an
634 influential feature whereby CIP molecules adhere to the nanocomposite surface because both the
635 adsorbent and adsorbate moieties contain a lot of oxygen and hydrogen rich functional groups. The
636 possibility of regeneration and reusability of nanocomposites opens up enormous possibilities for
637 low-cost, long-term sorbent material development for pharmaceutical pollution management.

638 Januário et al., (2022) recently reported on the use of GO functionalized activated carbon (GAC-
639 GO) for the efficient uptake of pharmaceuticals for COVID-19 treatment from water. This study
640 aimed to remove water contaminated with chloroquine and dipyrone using batch adsorption
641 processes. In this study, the authors discovered that the equilibrium time for chloroquine and

642 dipyrone adsorption was 18 and 12 h, respectively. The adsorption of chloroquine and dipyrone
643 onto GAC-GO fits the Langmuir model best and follows pseudo-second order. Thermodynamic
644 studies revealed that the process is endothermic, with adsorption capacity of 37.65 and 62.43 mg/g
645 at its peak at 318 K, respectively. The main mechanism of the underlying adsorption process was
646 attributed to hydrogen bonds and π -interactions between chloroquine and GAC-GO.

647 Mortazavi et al. (2019) reported that GO was simultaneously subjected to thermal reduction and
648 chemical bonding on the surface of amino-functionalized sand particles (AFSPs) and was
649 employed to adsorb naphthalene and acenaphthene from aquatic environments. The experimental
650 data were fitted to the Langmuir, Redlich-Peterson, and Dubinin-Radushkevich models for
651 naphthalene adsorption, and the Redlich-Peterson and Freundlich models for acenaphthene
652 adsorption, according to the equilibrium results analysis. The kinetic studies reveal both
653 adsorbate's adsorption process proceeds the pseudo-second-order and intra-particle diffusion
654 models. Naphthalene and acenaphthene had maximum adsorption capacities of 7.473 and 18.152
655 mg/g, respectively. Adsorption mechanisms in this study includes π - π stacking and hydrophobic
656 interactions: during thermal reduction, GO lose most of its functional groups, and amino-
657 functionalized sand particles were coated with rGO as a hydrophobic layer which promotes
658 hydrophobic interaction between rGO and the adsorbates (naphthalene and acenaphthene). The -
659 stacking mechanism is another adsorption mechanism that could be responsible for adsorption
660 capabilities.

661 Zhang et al., (2022a) outstanding polyvinylidene fluoride (PVDF)-PB-graphene oxide (GO)
662 adjusted membrane was synthesized through phase inversion for a small amount radio-nuclide
663 cesium (^{137}Cs) adsorption from wastewater. The authors reported that integration of GO increased
664 PB diffusivity, and the PVDF-PB-GO membrane displayed the largest Cs^+ uptake effectiveness of
665 99.6 %. Moreover, the membrane displayed conspicuous selectivity and reusability towards small
666 quantity of radioactive cesium, even in the presence of extreme co-existing ions and in real water,
667 which showed convincingly that the membrane has potential for usage. Two pathways were
668 suggested to account for Cs^+ adsorption behavior unto modified PVDF-PB-GO membrane. Firstly,
669 the XPS survey revealed that the N-Fe binding of PB was replaced by $\text{C}\equiv\text{N}\cdots\text{Cs}^+$ with the
670 elimination of $\text{Fe } 2p^3$ after adsorption suggesting that $\text{Fe}(\text{CN})_6^{4-}$ defect sites could as well be active
671 adsorption sites. Furthermore, the adsorption of Cs^+ can also be attributed to oxygen containing

672 surface functional groups (O—H group and C=O stretch) on the surface of GO as evidenced by
673 FT-IR spectra analysis.

674 Ma et al., (2017) investigated the utilization of GO membrane in the adsorption of Cs(I) and Sr(II)
675 from wastewater. The authors observed that Cs(I) and Sr(II) ions diffused quickly through
676 graphene oxide membranes, but the lanthanide ions and actinide ions are slower, making them to
677 separate based on the variation in hydrated ionic radii. Furthermore, the initial metallic ion
678 concentrations and acidity in the solution of the feed affected ion transport through the graphene
679 oxide membranes, larger concentrations of initial metallic ions and acidity of the feed solution
680 favored Cs(I) and Sr (II) adsorption.

681 In another recent study by Yang et al., (2021a), the sorption of radioactive waste U(VI) onto a
682 synthesized novel magnetic composite graphene oxide/Fe₃O₄/glucose-COOH (GO/Fe₃O₄/GC)
683 was investigated. At optimum adsorption conditions; an initial concentration of 10 mgL⁻¹, 5.0 pH
684 value, and sorbent dosage of 0.15 g/L, the maximum adsorption capacity was observed to be
685 (390.70 mg/g) at 30 mins of contact time. The observable higher U(VI) uptake and faster
686 adsorption rate when compared to previously reported studies was credited to abundant presence
687 of GO showing its effectiveness as an absorbent and potential for industrial use. Adsorption
688 behavior could be explained by the Dubinin–Radushkevich (D–R) model which fitted well with
689 the equilibrium data and showed a physical adsorption process taking place ($E < 8 \text{ kJmol}^{-1}$). While
690 the best fit for the adsorption kinetic parameter is pseudo-second order, indicating a high level of
691 complexation between U(VI) ions and organic functional groups observed on the as manufactured
692 nanocomposite.

693 ALOthman et al., (2022) fabricated γ -Cyclodextrin-graphene oxide nanocomposite for the
694 treatment of tetracycline and chlortetracycline antibiotics removal from aqueous environment. The
695 authors reported that the adsorption optimum conditions under studied were concentration of
696 400 mg/L, 30 min adsorbent time, pH 8.0, adsorbent dose 1.0 g/L and temperature of 278 K. The
697 adsorption of tetracycline and chlortetracycline was described best by the Freundlich model
698 suggesting a multilayer adsorption. The maximum percentage treatment of tetracycline and
699 chlortetracycline were found to be 91.25 and 93.75 % respectively. The adsorption process was
700 revealed to follow pseudo-second kinetic order reaction and liquid film diffusion kinetic model.

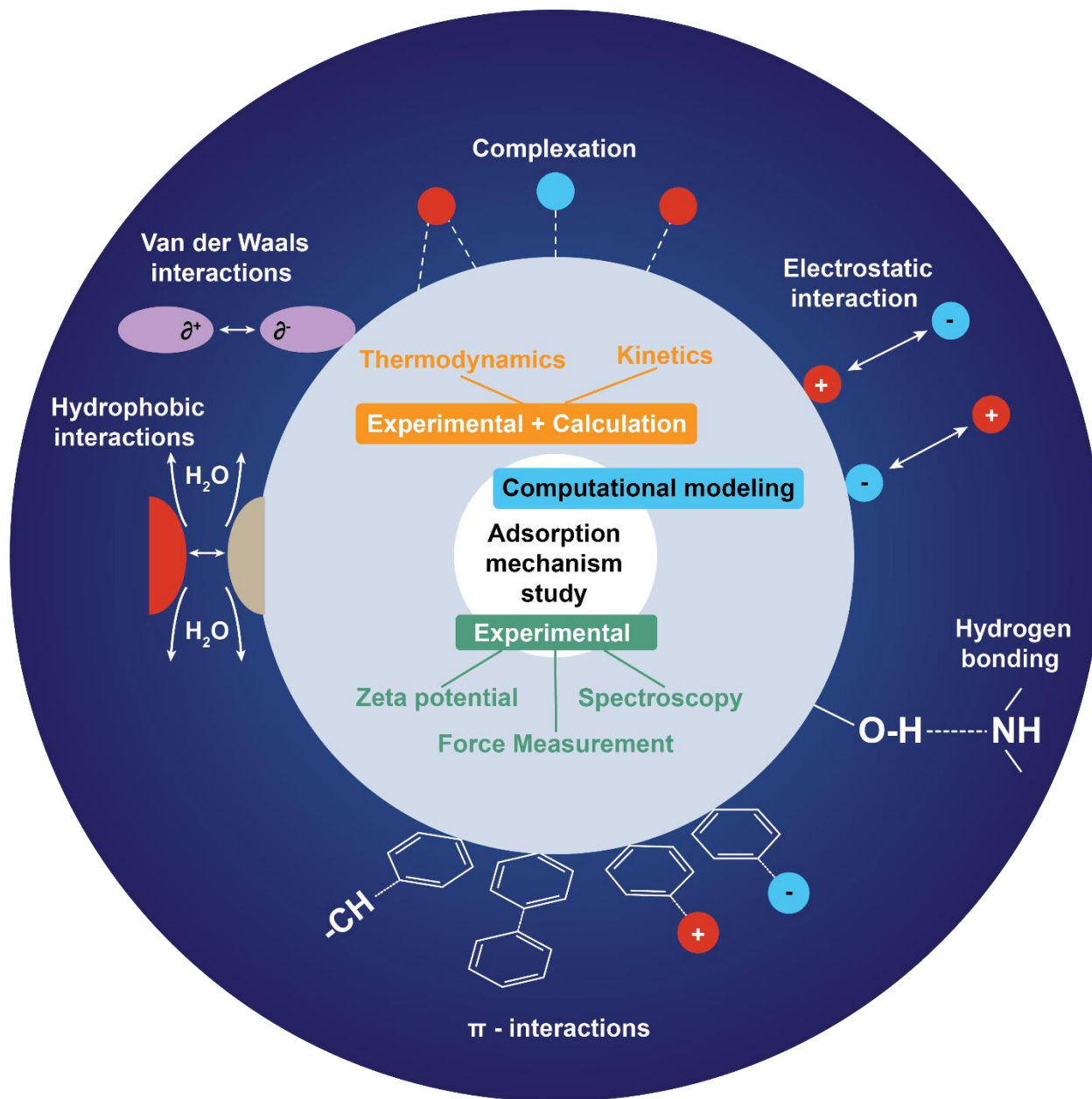
701 The thermodynamics study revealed degree of freedom increase, exothermic and spontaneous in
702 nature. The hydrogen bonding and π - π interactions were adsorption mechanism of adsorption.

703 The fabrication of copper nanoparticles immobilized- β -cyclodextrin modified reduced graphene
704 oxide (Cu/ β -CD/rGO) were developed successfully as an effective extractor of tetracycline (TC),
705 oxytetracycline (OTC) and doxycycline (DC) antibiotics from various aqueous environment was
706 explored by Yakout et al., (2021). The authors revealed that TCs are deposited strongly Cu/ β -
707 CD/rGO nanocomposite matrix via surface complexation with the Cu-nanoparticles besides the
708 formation of inclusion complexes with β -cyclodextrin and π - π interaction of reduced graphene
709 oxide. The maximum adsorption capacity of Cu/ β -CD/rGO evaluated from the Langmuir isotherm
710 model was found 403.2 mg/g, 476.2 mg/g and 434.8 mg/g for TC, OTC and DC respectively. It
711 was concluded that the prepared novel nanocomposite demonstrated a quick and highly effective
712 treatment performance for the antibiotic pollutant treatment.

713 Yang et al., (2022b) reported the synthesis of graphene oxide modified κ -carrageenan/sodium
714 alginate (GO- κ -car/SA) gel for the removal of Ciprofloxacin (CIP) and Ofloxacin (OFL). It was
715 revealed by the authors that GO nanosheets addition improves the mechanical strength and anti-
716 swelling property of the double-network hydrogel, making it possible for the application in the
717 fixed-bed column system. The maximum adsorption capacity calculated for CIP and OFL
718 adsorption onto GO- κ -car/SA gel were 272.18 and 197.39 mg/g. The authors also reported that the
719 GO- κ -car/SA gel was observed always to be negatively charged, suggesting that adsorption
720 capacity of the gel is better in an acidic environment.

721 Recently, Andrade et al., (2022) reported the preparation of graphene oxide (GO) anchored on iron
722 oxide nanoparticles ($\alpha\gamma$ -Fe₂O₃) and cobalt oxide (Co₃O₄) for the removal of caffeine in a batch
723 adsorption. The GO# $\alpha\gamma$ -Fe₂O₃Co₃O₄ adsorbent was reported to have demonstrated about 80v%
724 removal coupled maximum adsorption capacity of 28.94 mg/g. The adsorption kinetics as well as
725 the adsorption GO# $\alpha\gamma$ -Fe₂O₃Co₃O₄ was reported to follow a pseudo-second order kinetics and
726 better fitted to the Langmuir and Temkin models isotherms adsorption data. The thermodynamic
727 variables studied revealed that the adsorption process was exothermic, spontaneous and favorable.

728



729 Fig. 6. Insights into possible adsorption mechanism of biomedical waste onto graphene-based
 730 materials (Source: Wang et al., 2021a)
 731

732
 733 **6. Adsorption isotherm and kinetic studies**

734 Studies of isotherm and kinetics of adsorption experiment is a way of understanding probable
 735 mechanisms as well as pathways associated with the process. Generally, the adsorption isotherms
 736 refer to the quantity of pollutant adsorbed with the pollutant's concentration in the substrate at
 737 equilibrium. It is also needed to evaluate the adsorbent's efficiency for removing contaminants
 738 and investigate the surface properties (Xing et al., 2015). An earlier study of adsorption isotherms

739 shows the most frequently used isotherms are Freundlich and Langmuir isotherms as shown in
 740 Table 4 (Wang et al., 2017). The availability of several proved isotherms established on various
 741 assumptions and instances, the closest to the real case is fitted to the experimental data.
 742 Consequently, the study of the isotherms statistically is done to detect the models that depict and
 743 best fits the process of contaminants removal from effluents after analysis by several categories of
 744 nanoadsorbents (Ahmed et al., 2020).

745

746 Table 4. The most common isotherm model equations in adsorption

Models	Equation	Plot	Parameters	References
Langmuir	$\frac{C_e}{q_e} = \frac{1}{q_m K_L} + \frac{C_e}{q_m}$	$\frac{C_e}{q_e} vs C_e$	q_m, K_L	Langmuir, (1916)
Freundlich	$\log q_e = \log K_F + \frac{1}{n} \log C_e$	$\log q_e vs \log C_e$	$K_F, \frac{1}{n}$	Freundlich, (1906)

747

748 where q_m represents peak adsorption capability of metal ions (mg/g); K_L , the Langmuir isotherm
 749 constant (L/g); C_0 , and C_e are the initial concentration and concentration at equilibrium respectively
 750 (mg/L), k_f represents Freundlich constant in relation to adsorption capability, and n is the
 751 adsorption intensity. The Langmuir isotherm assumes that antibiotic molecules removal takes
 752 place on a uniform surface by monolayer adsorption with uniform binding sites, similar energy,
 753 and no movement between adsorbed species (Li et al., 2011). In contrast, Freundlich isotherm is
 754 an empirical model depicting heterogeneous surfaces (Zanin et al., 2017). The treatment process
 755 is favorable whenever $1/n$ in the Freundlich model equation is below 1 (Park et al., 2016). In the
 756 interpretation of adsorption, there exist differences in the effectiveness of Langmuir and
 757 Freundlich models. However, some of these models' variables such as excessive adsorption
 758 capacity (Langmuir) and constant linked to the distribution coefficient (Freundlich), have broad
 759 application in the characterization of the adsorption capacity for various species.

760 Graphene and its derivatives have risen as a novel material for usage as efficacious material to be
 761 applied in wastewater treatment. Due to their exceptional properties such as large number of
 762 functional groups, high surface area, and exceptional charge carrier mobility, Gr-based materials
 763 are exploited as sorbents for effluent decontamination.

764 Wu et al. (2013) reported the removal of doxorubicin hydrochloride from an aqueous solution
765 using GO. The authors found that the maximum adsorption capacity was 1428.57 mg/ and
766 concluded that the Langmuir model fit better experimental data than the Freundlich model.

767 Sulfamethoxazole (SMX) uptake by graphene oxide was studied by Nam et al. (2015). It was
768 discovered that Freundlich model had a better fit for the adsorption isotherm data than Langmuir
769 model based on the correlation coefficients. In the study of TC uptake using Fe₃O₄@SiO₂-
770 chitosan/GO (MSCG), the isotherms of adsorption were simulated with both Freundlich and
771 Langmuir equations. The authors revealed the appropriateness of Freundlich model more than
772 Langmuir for Tetracycline removal.

773 The removal of oxytetracycline (OTC) and TC by Fe₃O₄@G was investigated by Zhang et al.,
774 (2017). The result obtained showed higher correlation coefficient with the Langmuir model than
775 Freundlich model: Langmuir: R² =0.990 and 0.924, Freundlich: =0.986 and 0.921 for TC and OTC
776 respectively, suggesting a monolayer adsorption and uniform distribution of adsorption site.

777 Wang et al., (2020) investigated the effective adsorption of TC- hydrochloride antibiotics with
778 synthesized Zr-based MOF composite UiO-66-(COOH)₂/GO. The result obtained for R² when
779 compared showed that the experimental data best fits the Langmuir model (0.9935 < R² < 0.9967)
780 than Freundlich model (0.9401 < R² < 0.9872), revealing mono-layer mechanism of interaction
781 and uniform TC uptake on the MOF.

782 GO and GO-CMC (carboxymethylcellulose) nanomaterials were synthesized in films by
783 Juengchareonpoon et al., (2021). It was also restructured with citric acid crosslinks for adsorption
784 of antibiotics. The obtained results revealed maximum adsorption capability of 370.93, 256.68 and
785 102.05 mg/g for trimethoprim, oxolinic acid and oxytetracycline respectively at 30 °C.

786 Suksompong et al, (2021) studied the possibility of adsorbing iodine-131 from a hydrous solution
787 using GO/Chitosan sponges. The adsorption efficiency was studied making use of stable isotopes
788 and further studied using iodine-131 radioisotopes for confirmation of results. The experimental
789 data fitted well with the Langmuir model. The value of R_L (separated factor) obtained was between
790 0-1 substantiating the favourability of the adsorption of iodide using GO/Chitosan sponges with
791 maximum adsorptive capability of 0.263 MBq/mg.

792 ALOthman et al., (2022) also synthesized γ -Cyclodextrin-GO nanocomposite for the uptake of TC
793 and Chloro-TC antibiotics from water. The authors revealed that the sorption followed Langmuir
794 model. The highest percentage removal of TC and Chloro-TC were 91.25 and 93.75 %
795 respectively, at different pH values.

796 Feng et al., (2022) developed novel GO/COF-300/PPy sorbent via hydrothermal method to adsorb
797 indomethacin (IDM) and diclofenac (DCF) from water. The results reveal the adsorption capability
798 and uptake efficacy of indomethacin and diclofenac by GO/2COF-300/4PPy is high at 99% for
799 indomethacin and 97 % for diclofenac (115 mg/g and 138 mg/g respectively). The authors also
800 revealed that adsorption of indomethacin and diclofenac onto GO/2COF-300/4PPy conformed to
801 the Langmuir isothermal model.

802 Yang et al., (2022c) studied the removal of enrofloxacin (ENF) onto GO. The authors concluded
803 that the Langmuir-Freundlich model gave the best fit of adsorption process with an adsorption
804 capacity of 45.035 mg/g.

805
806 Adsorption kinetic models are highly crucial for predicting optimal conditions especially for batch
807 adsorption processes (Kyzas et al., 2018). Kinetic modeling gives robust interpretation concerning
808 adsorption forces/interactions which reveals the entire adsorption mechanism and potential rate-
809 controlling steps like mass transport or processes involving chemical reaction. Some widely
810 explored models include Pseudo-first and pseudo-second order, Elovich equation and intraparticle
811 diffusion (Awad et al., 2020). But recently the pseudo-first and the pseudo-second order are the
812 most explored kinetic model equations. The linear form equation of the models mentioned above
813 is depicted in Table 5. The pseudo-first order kinetic model physisorption as the basis of adsorption
814 process, occurring without any chemical bonding and only through weak Van der Waals forces.
815 The adsorption process is easily reversible which allows for a near effortless regeneration.
816 According to the pseudo-second order, two reactions occur either simultaneously or sequentially.
817 Given that the initial reaction is quick, it reaches equilibrium quickly. Meanwhile, the second
818 reaction proceeds steadily and takes longer to arrive at equilibrium (Wang et al., 2015). Adsorption
819 occurs via chemisorption, as indicated by the pseudo-second order. It is concluded that bonding
820 occurs as a result of electronic sharing, and that the transfer between adsorbents and adsorbate is

821 relatively stronger than the physisorption pathway from pseudo-first order kinetics (Ahmad et al.,
822 2020).

823

824 Table 5. The most common kinetic model equations in adsorption

Kinetic models	Linear form	Plot	Parameters	Reference
Pseudo-first-order	$\log (q_e - q_t) = \log q_e - \frac{k_1 t}{2.303}$	$\log (q_e - q_t)$ vs t	$q_{e,cal}, k_1$	Lagergren and Svenska, 1898
Pseudo-second- order	$\frac{t}{q_t} = \frac{t}{q_e} + \frac{1}{k_2 q_e^2}$	$\frac{t}{q_t}$ vs t	$q_{e,cal}, k_2$	Ho and McKay, 1999

825

826 where k_1 is the pseudo-first-rate constant (min^{-1}), k_2 is the pseudo-second order rate constant
827 (g/mgmin), q_e and q_t are the adsorption capacity at equilibrium and time, t (mg/g).

828 Understanding the kinetics of antibiotic adsorption on graphene graphene-based nanomaterials is
829 essential to the adsorption mechanism and spent graphene/graphene-based nanomaterials, which
830 is closely related to the diffusive state of graphene materials. Adsorption of antibiotics by graphene
831 oxide with good diffusivity is fast. GO with good dispersibility can adsorb antibiotics quickly, but
832 Gr and reduced graphene oxide (RGO) with low diffusive need more time to reach equilibrium (Li
833 et al., 2018).

834

835 Zhu et al. (2015) reported that Gr exhibited swift adsorption capability and attained equilibrium in
836 3 min, and the removal process fitted well into the pseudo-second-order kinetic model compared
837 to the pseudo-first-order model.

838

839 Song et al. (2016) discovered that the pseudo-second-order kinetic model better fitted the kinetics
840 of TC and sulfamethazine removal by reducing graphene oxides than the pseudo-first-order model.

841

842 Wang et al. (2016) reported a similar result using MCGO to remove CIP. These facts suggest
843 antibiotics removal by graphene/GBNPs is mainly controlled by chemical adsorption through the
844 exchange or pairing of electrons between adsorbates.

845 Hiew et al., (2019) investigated removal of diclofenac using graphene oxide (GO). The authors
846 reported PSO model as the optimal representation of the kinetic of diclofenac adsorption.

847

848 In another study, Ninwiwek et al., (2019) prepared mesoporous silica-magnetic graphene-oxide
849 nanocomposite material (mGO-Si) for the uptake of sulfamethoxazole (SMX). The results shows
850 the mGO-Si removed the sulfamethoxazole molecules more efficiently than the pristine magnetic-
851 GO with the Kinetic data exhibiting good correlation based on the PSO model.

852
853 Radmehr et al., (2021) displayed the production and efficient deployment of renewable sorbents
854 based on GO (i.e., NiZrAl-layered double hydroxide-graphene oxide-chitosan (NiZrAl-LDH-GO-
855 CS NC)) for Nalidixic acid uptake. The kinetics of the Nalidixic acid being adsorbed on LDH-
856 GO-CS was examined by the authors using PFO kinetic model, the pseudo-PSO, IPD and Elovich
857 mechanism and discovered the R^2 values are positioned between 0.9884–0.9966 giving a well
858 fitted Nalidixic acid removal by LDH-GO-CS NC as shown by the pseudo second order model.

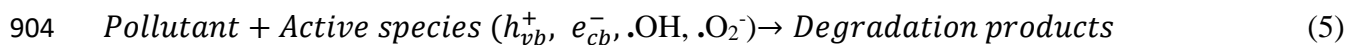
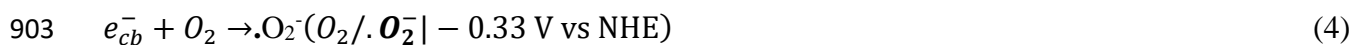
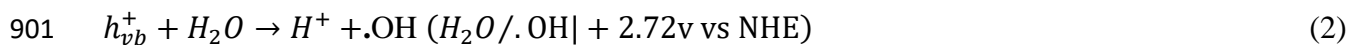
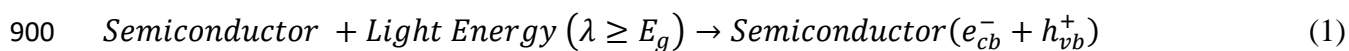
859
860 Zou et al., (2021) reported the one-pot fabrication of $-Fe_2O_3$ nanoparticles growth on RGO for the
861 adsorptive uptake of chlortetracycline, tetracycline, and oxytetracycline. The authors reported that
862 the adsorption of chlortetracycline, tetracycline, and oxytetracycline onto $-Fe_2O_3 @RGO$
863 nanocomposites take 20 min and is highly pH-dependent because of the enhanced repulsive
864 interaction at high and low pH, and that the adsorptions fit well the PSO equations.

865
866 Jaswal et al., (2021) also reported the utilization of rGO-MoS₂heterostructure for the treatment of
867 ofloxacin from the aqueous phase. It was found from the result that the adsorption of ofloxacin
868 onto rGO-MoS₂ followed pseudo-second order kinetics.

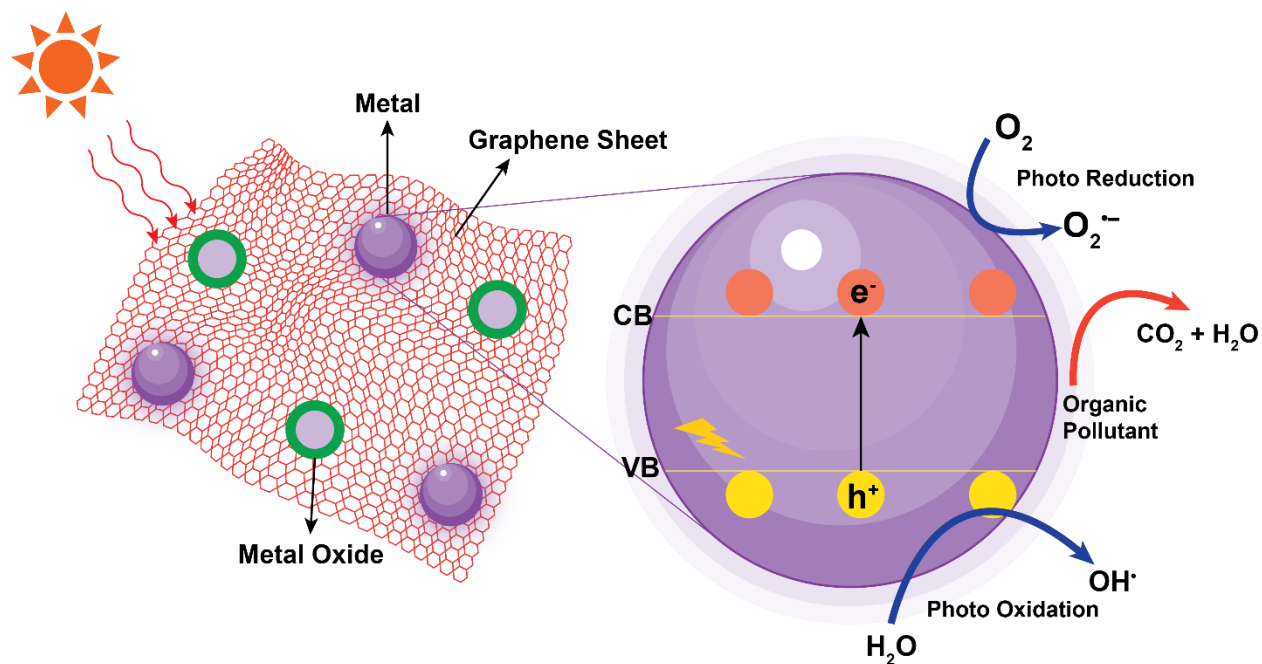
869 870 7. Photocatalytic degradation of biomedical waste

871 Several chemical treatment methods such as ozonation, chlorination, and Fenton's oxidation have
872 undergone developments for removing antibiotic remains from wastewater. However, difficult or
873 extensively prolonged process in obtaining total decomposition and possible destruction of
874 desirable organisms because of their low selectivity leading to undesirable losses are major
875 drawbacks to these methods (Yang et al., 2021b). In addition to the above, the process incurs high
876 economic capital and operational cost. Although integration of physical processes substantially
877 reduces the noxiousness of water containing antibiotics after treatment, it is a rather knotty and
878 expensive process (Homem and Santos, 2011). Sequel to adsorption, active groups such as -OH,
879 $-O_2$ present in sunlight, visible light or UV light released by photocatalysts are used to disintegrate

880 antibiotics into unharmed quantities efficiently. Therefore, photocatalytic decomposition is one of
881 the high-ranking processes for removing antibiotic contaminants from the environment due to its
882 high efficiency and sustainability (Saher et al., 2020). As a result of its exceptional advantages
883 such as its powerful redox potential, no adsorption engorgement, the possibility of totally
884 degrading organic contaminant into unharmed inorganic matter (e.g. CO₂ and H₂O),
885 inexpensiveness, mild reaction conditions (close to room temperature and atmospheric pressure),
886 extraction of oxygen in air for the production of highly potent oxidants and solar radiation energy;
887 photocatalysis possesses extensive prospect of application in environmental reclamation (Elmolla
888 and Chaudhuri, 2010). Therefore, photocatalysis has progressively attracted global interest and
889 broad application in novel energy extraction and techniques for environmental control. The
890 fundamental principle of Photodegradation is the excitement and movement of electrons from their
891 valance band into the conduction band after exposure to radiation with energy higher than its
892 optical band gap which produces equal quantity of positively charged holes in the valance band
893 (Xu et al., 2019). When the potential of the valance band vs normal hydrogen electrode (NHE)
894 exhibits higher positivity than H₂O/.OH (+272 V vs NHE) or, OH⁻/.OH (+189 V vs NHE) and the
895 potential of conduction band vs NHE is more negative than O₂/.O₂⁻ (-0.33 V vs NHE), the
896 semiconductor will be able to generate .OH and.O₂⁻. Thereafter, separation and migration to the
897 semiconductors surface of the photoinduced electrons and holes occurs and redox reactions will
898 take place at the reactive site on the semiconductor surface. The mechanism of semiconductor
899 photocatalysis reaction (Fig. 7) is given by the equations (Zhao et al., 2018; Yang et al., 2021b).



905



906

907 Fig. 7. Graphical illustration of photocatalytic reaction mechanism (Source: Ramalingam, et al.,
908 2022)

909 High surface area for homogeneous diffusion, thin band gap vitality alongside unique
910 electroconductivity in reposition and swift electron transport and minimal expenditure for large
911 scale production makes graphene a prospective photocatalyst and has been extensively used for
912 photocatalytic decomposition of antibiotic pollutant in water (Li et al., 2019). Nonetheless,
913 catalytic activities are easily lost by graphene planes during its self-accumulation process (Julkapli
914 and Bagheri, 2015) and research reveals the inability of GO, a significant component of graphene-
915 based nanomaterials to function under visible light as a result of low (1.79 eV) band gap
916 (Anirudhan 2017). This necessitates the combination of graphene with different photocatalysts to
917 produce new graphene-based photocatalysts to overcome these disadvantages and enhance the
918 catalytic operation of antibiotics. Recently, several steps have been taken to manufacture and
919 produce graphene-based photocatalyst to enhance their capability to decompose antibiotic
920 pollutants. Examples are single-semiconductor, coupled semiconductor, metal-coated single
921 semiconductor, and metal-coated coupled-semiconductor. Single-semiconductors include metallic
922 compounds and organometallic model such as Titanium oxide, Bi-based oxides, Zinc oxide, silver
923 tetraoxophosphate and many more. they have been used to photocatalytically decompose organic
924 contaminants. The metal-based hybrid nanocomposites material is redox capable and has a high
925 charge separation efficiency. All of these factors are critical for the efficient photocatalytic

926 breakdown of organic contaminants. Figure 4 depicts the photocatalytic mechanism of a
927 metal/metal oxide decorated graphene sheet for organic pollutant degradation. Mohamed et al.,
928 (2021) found that the multifunctional effects of Ag, CA, and GO on the structural characteristics
929 of the graphene-based composite increased the photocatalytic activity of Ag-CdSe/GO/CA
930 nanocomposites. According to the authors, GO acts as an electron acceptor, increasing the
931 effectiveness of removing photo-generated carriers as well as the combined composite carrier.

932 Perera et al. (2012) created TiO₂ nanotube/reduced graphene oxide composites using an alkaline
933 hydrothermal technique. The photocatalytic activity of the composites was shown to be highly
934 influenced by the rGO/TiO₂ ratio. Due to its high surface area and excellent electron/hole
935 separation, the composite with 10% rGO had the highest photocatalytic activity, with a threefold
936 improvement in photocatalytic efficiency over pure TiO₂ nanotubes under UV and visible light.

937 Pan et al. (2012) employed the application of hydrothermal method to fabricate GO/TiO₂
938 nanowires and nanoparticles. TiO₂ nanowires disperse more uniformly on graphene with less
939 agglomeration than TiO₂ nanoparticles, resulting in more direct contact between TiO₂ and
940 graphene and thus enhanced electron-hole pair separation and transportation. As a result, GO/TiO₂
941 nanowires outperform GO/TiO₂ nanoparticles, pure TiO₂ nanowires, and TiO₂ nanoparticles in
942 terms of relative photocatalytic activity.

943 The combination of graphene materials with coupled-semiconductors have become a research area
944 of focus because it usually possesses extensive benefits of improving the disintegration of electron-
945 hole pairs and retaining oxidation and reduction at two separate sites for reaction (Tang et al.,
946 2015). Composite photocatalysts NeZnO/ CdS/GO was produced via a simplified hydrothermal
947 process by Huo et al., (2016). The composite showed significant photocatalytic activities.
948 Preparation of hetero-junction photocatalyst (Ag₃PO₄/BiVO₄/RGO) was a success through a
949 simplified in-situ deposition process. Tayel et al (2018) discovered that coating TiO₂ with graphene
950 oxide increased the TiO₂ catalytic activity by a factor of 1.2. The primary photocatalytic activity
951 of TiO₂ resulted from the electron acceptance and GO transport (Zhang et al., 2020). The electrons
952 accepted by GO were produced on the TiO₂ surface in the presence of light, which reduces
953 electron-hole recombination and increases the production of active holes (Ajala et al., 2022).
954 Another reason for the increased titanium oxide photocatalytic activity was the reduction in the

955 width of the TiO₂ band gap caused by the GO addition. This band gap narrowing allows the
956 photocatalyst to produce radicals at elongated wavelengths. Several researchers have recently
957 considered integrating two or more metallic oxides with GO as a potential method for increasing
958 catalytically enhanced activity when organic pollutant begin to degrade.

959 Xu et al., (2020) investigated the photocatalytic degradation activities of ciprofloxacin (CIP),
960 norfloxacin (NOR) and tetracycline (TC) over a series of rGO/Bi₄O₅Br₂. The authors revealed
961 from the results obtained that photodegradation of these target antibiotics almost never be possible
962 without adding any photocatalysts. The photodegradation of these antibiotics was successfully
963 commenced by using Bi₄O₅Br₂ nanosheets and rGO/Bi₄O₅Br₂ nanocomposites as photocatalysts.
964 As expected, the degradation efficiency of each target antibiotic at any rGO/Bi₄O₅Br₂
965 nanocomposites is greater than that of Bi₄O₅Br₂ nanosheet. Bi₄O₅Br₂ on the surface of the
966 rGO/Bi₄O₅Br₂ nanocomposites can be excited to produce electrons (e⁻) and holes (h⁺) when
967 illuminated by simulated sunlight. The photogenerated holes can react efficiently with the target
968 antibiotics pollutant to degrade them, and to remove the photogenerated electron-hole pairs
969 effectively. As a result of their excellent electron reservoir capability of rGO and conductivity,
970 photogenerated electrons can be transferred quickly to the rGO/Bi₄O₅Br₂ nanocomposite surface
971 to reacted with O₂, thus generating .O₂⁻ radicals. Meanwhile, The instantaneous formation of .OH
972 by the reaction of .O₂ radicals and H⁺ is also possible. Following that, .O₂ and .OH radicals can
973 oxidize the target antibiotics adsorbed on the surface of the rGO/Bi₄O₅Br₂ nanocomposite to
974 complete the photodegradation process.

975 Fakhri and Bagheri, (2020) reported the fabrication of UiO-66@WG for the photocatalytic
976 degradation tetracycline (TC) and malathion (MA). It was clearly reported by the authors that after
977 photocatalytic efficiency of 84 and 100 % was achieved for TC and MA respectively, by UiO-
978 66@35WG as an optimum photocatalyst after 70 min of irradiation. The UiO-66@35WG showed
979 enhanced response to visible light, better separation of charge carriers, good contacting between
980 energy levels of components, and more availability of active site that are responsible for its
981 superior photodegradation efficiency in compared with pristine UiO-66. The photocatalytic
982 mechanism verified that O₂⁻ is main radical species involved in this process. Finally, the authors
983 concluded that precise positioning of energy levels belonging to components and the formation of

984 an electrical field results in effective charge transfer and enhanced separation of electron-hole
985 pairs, which is advantageous in a photocatalytic system.

986 Wang et al., (2022) explored the fabrication of magnetic cobalt ferrite/reduced graphene oxide
987 (CF/rGO) porous balls for effective photocatalytic degradation of oxytetracycline. It was revealed
988 that enhanced adsorption makes it easier for the photocatalyst to have strong interaction with OTC,
989 thereby improving the degradation efficiency. Under visible light irradiation ($\lambda > 420$ nm), the light
990 excited CF/rGO-0.2 to produce electron-hole pairs. h^+ exhibits strong oxidation capacity and can
991 directly oxidize OTC. At the same time, electrons are captured by rGO, which effectively reduces
992 the charge carrier recombination. In addition, the unique porous balls increase the light absorption
993 capacity and provided more catalytic centers. Therefore, CF/rGO showed good photocatalytic
994 activity in photocatalytic redox reaction with 84.7 % degradation efficiency. The trapping
995 experiments revealed that holes (h^+) and superoxide radicals (O_2^-) played a crucial role in the
996 degradation of OTC, implying a possible photocatalytic reaction mechanism.

997 The photocatalytic degradation of Tetracycline (TC) under visible-light using by reduced graphene
998 oxide decorated MoO_3/TiO_2 nanocomposite was investigated by Ali et al., (2022). According to
999 the authors, RGO decreases electron-hole pair recombination by functioning as an acceptor of
1000 photo-generated electrons from TiO_2/MoO_3 nanoparticles. As a result, it generates even more
1001 photo-generated holes, promoting the formation of reactive oxygen species and pollutant
1002 degradation. Surface imperfections on the TiO_2/MoO_3 surface of the RGO can retain electrons in
1003 this case, and the intermediate product can then replicate surface defects via interfacial charge
1004 transfer. The presence of defects that act as trapping centres can extend the lifetime of electrons or
1005 holes in metal oxide coupling, and photocatalytic activity rises as RGO concentration increases.
1006 The authors also reported that the excellent photo-degradation impact of TC via the $Gr/MoO_3/TiO_2$
1007 was due to the synergetic (interfacial) interaction of the graphene sheets and the MoO_3/TiO_2 .
1008 Furthermore, the MoO_3/TiO_2 was utilized as a migration vehicle for the visible light carrier, while
1009 the decreased graphene sheet's large surface area and number of active sites increased
1010 photocatalytic activity with almost 94 % TC photodegraded during 80 min under visible light
1011 irradiation.

1012 Zhang et al., (2022b) studied the photodegradation performance tetracycline (TC) onto PG/TiO₂
1013 under UV and visible light. The authors observed that TiO₂ photocatalytic activity was discovered
1014 to be closely linked to its surface phase, and the creation of a surface-phase junction between
1015 anatase and rutile may facilitate spatial charge separation. It was also observed that the PG might
1016 shift the light absorption edge from UV to visible light, resulting in additional photogenerated
1017 electron holes. Furthermore, there was a dual effect resulting from TiO₂ and PG combination
1018 which involves the enhancing adsorption of visible light while also improving the separation
1019 ability of e⁻ and h⁺ to significantly inhibit e and h⁺ recombination. The authors' proposed adsorption
1020 and photocatalytic mechanism is that, first, as an effective absorbent during dark conditions, the
1021 PG and TiO₂ reactive interface would adsorb a large amount of TC molecules to the material's
1022 surface and into the confined area. Second, under visible and UV light, TiO₂ was bombarded with
1023 energy higher than the band gap, while electrons (e⁻) in the valence band could absorb the photon
1024 energy causing them to migrate to the conduction band and form electropositive holes (h⁺) in the
1025 valence band. Thirdly, to prevent charge recombination, h⁺ and e⁻ moved from the interior to the
1026 surface of PG, and the interface functioned as the activity sites. By interacting with H₂O, h⁺
1027 produced ·OH, and electrons on the surface of PG/TiO₂ produce ·O₂⁻ by absorbing ·O₂⁻. Lastly, the
1028 photocatalytic process involving active species (·O₂⁻, h⁺, and ·OH) were involved in in redox
1029 reactions which were responsible for the removal of TC via degradation of its molecules to form
1030 smaller organic molecules, CO₂ and H₂O.

1031
1032 Ghorbanih and Salem, (2021) reported the performance of hybridized materials containing
1033 graphene oxide and carbon nanotubes (CNTs) to photocatalytically treat sewage released out of an
1034 industrial estate. Their findings revealed the capability of hybridized nanocomposites to treat the
1035 accumulated sewages at various steps of the industrial recovery process, between the anaerobic
1036 system and the sand filter. The suitable distribution ratio of graphene and CNTs were calculated
1037 to be 3.33 %. The end-result of parameters such as initial COD, period of irradiation, sewage
1038 collection position, as well as pH on treatment performance were investigated. The maximum
1039 photo-activity was reached in 20 min by keeping the pH of the sewage at 8. The authors consider
1040 larger surface area, of 60 m²/g and lower band gap energy of 2.1 eV as responsible.

1041 Ag₃PO₄-graphene and Ag₃PO₄-graphene/Ag was synthesized by Zhou et al. (2016) via chemical
1042 precipitation for the decomposition of sulfamethoxazole. Under synthetic solar radiation, 1ppm of

1043 sulfamethoxazole was almost totally degraded in 30 min using the two photocatalysts. The
1044 integration of Ag on Ag_3PO_4 -graphene did not show any reasonable upgrade in its Photocatalytic
1045 functionality for sulfamethoxazole decomposition as compared to its pure form. The contribution
1046 of the Ag load is therefore unclear and subject to further research. Hetero-junction composites.

1047 Cao et al. (2016) found that photocatalytic degradation of tetracycline using magnetic-GO/Ce/TiO₂
1048 degraded 82.9 % of the tetracycline. Priya et al. (2016) also accounted that ampicillin and
1049 oxytetracycline were photocatalytically degraded by Bi₂O₃/BiOCl reinforced on chitosan and
1050 graphene-sand composite, with 95 % ampicillin removal attained in 1 h solar light (Ajala et al.,
1051 2022).

1052 The photocatalyst revealed 90% TC adsorption under visible light radiation (Chen et al., 2017).
1053 This is higher than those obtained from BiVO₄, $\text{Ag}_3\text{PO}_4/\text{BiVO}_4$, and RGO/BiVO₄ which showed
1054 56, 82 and 78 % adsorption respectively.

1055 Wang et al. (2017) successfully developed a $\text{C}_3\text{N}_4/\text{MnFe}_2\text{O}_4$ /graphene composite for antibiotic
1056 degradation. The four antibiotics studied were metronidazole, amoxicillin, tetracycline, and
1057 ciprofloxacin, and $\text{C}_3\text{N}_4@\text{MnFe}_2\text{O}_4$ -graphene composites removed 94.5 % of metronidazole,
1058 which was approximately 3.5 times greater than pure g- C_3N_4 .

1059 Guan et al., (2021) successfully fabricated Z-scheme photocatalyst for TC-hydrochloride
1060 decomposition using Bi₂WO₆ nanosheets, graphene oxide, and silver bromide nanomaterials. The
1061 modified Z-scheme composite (15 %AgBr/5GO/Bi₂WO₆ (15A/5G/BW) showed increased
1062 intersurface charge separation and transmission because of GO's exceptional electrical
1063 conductivity. Consequently, 15A/5G/BW showed the best TC-hydrochloride photocatalytic
1064 activities. Under visible light radiation, the peak decomposition effectiveness of 84 %, and the
1065 kinetic constant was found to be greater at 0.0515 min (approximately 4.60 and 3.16 times) than
1066 that of AgBr and Bi₂WO₆, respectively.

1068 BiOBr/MoS₂/Graphene oxide (Bismuth-oxybromide/molybdenum disulfide/GO) fabrication was
1069 reported used by Li et al., (2021) to modify the capability of photocatalytic decomposition and
1070 adsorption of oxytetracycline (OTC). The composites exhibited an excellent photocatalytic
1071 functionality for oxytetracycline decomposition. In the presence of visible light radiation,
1072 oxytetracycline, doxycycline, chloro-TC were spontaneously adsorbed with over 98 %
1073

1074 decomposition rate in 40 min. Further studies can be undertaken taking into consideration the
1075 benefits of ion-doping and coupled-semiconductors towards improving Photocatalytic activity and
1076 graphene composite synthesis.

1077 Alamgholiloo et al., (2021) fabricated a novel and effective GO/CuBDC-Fe₃O₄ ternary
1078 nanocomposite for ciprofloxacin (CIP) degradation. According to the authors, the ternary
1079 nanocomposite demonstrated the highest CIP degradation rate (98.5 %) in 24 min, with a rate
1080 constant of 0.191 min⁻¹. The results showed that Cu/Fe species and C=O groups in ternary
1081 nanocomposite catalyzed PMS to the generation of hydroxyl and sulfate radicals for CIP
1082 decomposition. Moreover, the ternary nanocomposite demonstrated a high possibility of
1083 regeneration, allowing the catalyst to be easily separated from reaction mixtures with an external
1084 magnet. However, radical quenching tests and electron paramagnetic resonance (EPR) showed
1085 that hydroxyl and sulphate ions play an important part in the decomposition process.

1086
1087 According to Hsieh et al., (2022), recent advances have been made in the treatment of wastewater
1088 from industrial and medical sector. Untreated antibiotics, which are easily seen in effluents
1089 released by hospitals and manufacturers alike, have drawn the attention of environmentalists. The
1090 authors developed graphene quantum dot/ZnO composites that were used as a photocatalyst for
1091 metronidazole degradation. The results revealed an ultra-high removal efficiency (100 %) and a
1092 substantially increased reaction rate constant that was 1.74 times above the pristine sample. In
1093 summary, N-GQDs improve visible-light absorption and increase photo-induced charge carriers.
1094 This is due to the N-functionalized GQDs having a smaller optical band gap (3.0 to 3.5 eV) thereby
1095 propelling charge transfer in the heterostructure, improving photocurrent generation, and
1096 restricting electron-hole recombination from pristine ZnO crystals exposed to UV light.

1097

1098 **8. Recyclability of graphene-based nanomaterials**

1099 Due to its low economic cost and environmental sustainability, graphene has been widely applied
1100 in industrial applications. High quality product yield at minimal cost implication is a major
1101 consideration in any industrial process. However, as compared to lab-scale conditions, the
1102 industrial application is tougher and more complex. The stability and reusability of graphene must
1103 therefore be high for it to be considered for continuous process development for industrial
1104 application (Das et al., 2018). A major advantage of graphene-based nanomaterials is their

1105 stability, recyclability, and ability to regenerate from a solution. High adsorption capability
1106 should not be the only criteria for an excellent adsorbent but also outstanding desorption capacity
1107 which will significantly increase the effectiveness and reduce operational cost. Therefore,
1108 reusability and desorption are pertinent for graphene-based nanomaterials to be applied
1109 commercially (Peng et al., 2017). Graphene-based adsorbents must be subjected to separation from
1110 the medium, regeneration and recycling after utilization in effluent decontamination. The small
1111 particle size of these sorbents makes it difficult and strenuous to separate (Verma and Nadagouda,
1112 2021). Although RGO is derived from GO, it differs significantly from GO in terms of
1113 thermophysical properties. As a result of the oxygen-containing functional groups present in GO,
1114 phonon scattering occurs, resulting in extremely low thermal conductivity of GO. However,
1115 oxygen-containing functional groups can be removed to some extent, and thermal conductivity
1116 will be increased following the reduction process (Zhou et al., 2022). Several methods have been
1117 deployed to efficiently separate graphene-based sorbents from wastewater, among which the most
1118 handling is centrifugation, crossflow filtration, field-flow fractionation, and electric field (Ali et al.,
1119 2018; Kim et al., 2006).

1120 Mu et al. (2017) also described the development of 3-Dimensional nanostructured composite
1121 sorbents of RGO and WO_3 (RGO/ WO_3) for the removal of strontium ion (Sr^{2+}) from aqueous
1122 solutions. Adsorption isotherms reveal the experimental data well fitted the Langmuir isotherm (R
1123 > 0.99), and the peak adsorption capability of 149.56 mg/g was attained, which is greater than
1124 that of GO, WO_3 , and other close-related sorbents. Treatment of Sr^{2+} by RGO/ WO_3 attained
1125 equilibrium in 3h, 20min. The abundant treatment sites made available by the diffused WO_3
1126 nanoparticles on the Reduced Graphene Oxide surface made treatment rate faster and higher for
1127 RGO/ WO_3 . Moreover, the presence of sodium ions has no discernible impact on the adsorption of
1128 Sr^{2+} ions on RGO/ WO_3 , and the adsorption-desorption experiment with RGO/ WO_3 sorbent is
1129 recyclable at least 5 times without substantial adsorption capability loss.

1130 Xiao et al., (2019) investigated desorption of antibiotics from prepared molybdenum di-sulfide
1131 graphene-oxide supported magnetic nanoparticles ($\text{Fe}_3\text{O}_4/\text{GO}/\text{MoS}_2$) using Acetonitrile (CAN) as
1132 eluent. Desorption was obtained as 90.2, 87.8 and 85.6 % for Pazcofloxacin, Lecofloxacin, and
1133 Gatifloxacin respectively. They also carried out reusability tests under ideal conditions. The study's

1134 findings revealed that the $\text{Fe}_3\text{O}_4/\text{GO}/\text{MoS}_2$ material could be reused 10 times without significant
1135 loss.

1136 Qiao et al., (2020) synthesized MGO/ZnO nanocomposites (MZ) which was used in the removal
1137 of tetracycline (TC). The maximum adsorption capability of $1590.28 \text{ mg g}^{-1}$ observed in their
1138 study. Recyclability studies showed that MZ could be recycled up to four times with no apparent
1139 decrease in photocatalytic activity resulting from incomplete desorption of TC.

1140 Alamgholiloo et al., (2021) used a green solvothermal technique to fabricate a novel ternary
1141 nanocomposite ($\text{GO}/\text{CuBDC}-\text{Fe}_3\text{O}_4$) which was employed in degrading ciprofloxacin (CIP)
1142 antibiotic. A 98.5% removal rate was observed for CIP and still showed good degradation
1143 capability after four cycles, signifying the stability of the catalyst.

1144 The synergistic effect of magnetic particle coupling with graphene or GO can be the panacea to
1145 resolving the challenges that graphene separation poses. According to Bulin et al., (2020) and Ma
1146 et al., (2021), magnetization enables the practical use of GO in the production of adsorbents This
1147 is because very little energy is required which can be achieved by the use of an external magnetic
1148 field to provide excellent separation (Wang et al., 2021). The high chemical stability of Magnetic-
1149 graphene oxide (MGO) and its nanocomposites make it desirable and gradually position itself as
1150 an emergent and efficient treatment technology. The efficacy of MGO has been studied and can
1151 be used extensively in treating aqueous biomedical effluents including radionuclides and
1152 antibiotics- a contaminant of emerging concern. Moreover, MGO has good hydrophilic and
1153 magnetic properties and has been observed to be more stably dispersed in aqueous solution. In
1154 addition, it reduces the chances of severe agglomeration and nanosheet restacking, allowing for
1155 easy solid-liquid separation process. MGO is created by modifying magnetic materials such as
1156 ferric oxide to GO (Wang et al., 2021b). MGO can be made reusable by treatment mineral acids
1157 and bases (at low concentration), such as HCl, HNO_3 NaOH and sodium carbonate. The capacity
1158 for adsorption and regeneration is equal or even greater than other sorbents when compared.

1159 Ullah et al., (2022) synthesized reduced-MGO/polyaniline (RmGO/PANI) as a sorbent for the
1160 adsorption of moxifloxacin (MOX) and ofloxacin (OFL) from the aqueous samples. They achieved
1161 adsorption efficacy of 99% for MOX and 96 % for OFL. The adsorbent was reused repeatedly 10
1162 times maintaining an excellent removal capacity.

1163 Shi et al., (2020) synthesized CdS/reduced graphene (rGO)/ZnFe₂O₄ (ZFO) nanocomposite
 1164 system to attain efficacious Photo-Fenton decomposition of tetracycline (TC) in the presence of
 1165 visible light radiation. The authors found out that CdS/rGO/ZFO composite material adsorbed 80
 1166 % of TC mineralized at a 59.2 % in 1 hour, attributable to the photo-Fenton synergistic effect in
 1167 CdS/rGO/ZFO with the capacity of producing and degrading H₂O₂. Meanwhile, the CdS/rGO/ZFO
 1168 photocatalyst's prominent magnetic recovery property ensured economic benefits. The
 1169 CdS/rGO/ZFO adsorbent was reused after 4 cycles. The Recyclability of graphene-based
 1170 nanomaterials based on cycle of used with various biomedical pollutants is presented in Table 6.

1171 Table 6: Recyclability of graphene-based nanomaterials based on cycle of used.

Graphene nanocomposite	Pollutant/removal condition	Eluent used	Recovery	Cycle of used	References
MGO/ZnO* nanocomposites (MZ)	Tetracycline 100 min 1590.28 mg g ⁻¹	NaOH	80 %	4	Qiao et al., (2020)
Co-Fe-PBAs@rGO*	Levofloxacin Hydrochloride	-	83.7 %	5	Pi et al., (2018)
GO/CuBDC-Fe ₃ O ₄	ciprofloxacin (CIP) 98.5%			4	Alamgholiloo et al., (2021)
GOMPs	Tetracycline 10 min 98%	Ethanol		5	Lin et al., (2013b)
RmGO/PANI	moxifloxacin (MOX) – 99% ofloxacin (OFL) – 96 %		-	10	Ullah et al., (2022)
Fe ₃ O ₄ /GO/MoS ₂	Pazcofloxacin- 90.2% Lecofloxacin- 87.8%, Gatifloxacin- 85.6%	ACN		10	Xia et al., 2019
Cds/rGO//ZFO	Tetracycline 60 min 80%			4	Shi et al., 2022
AgFeO ₂ /GO	Lomefloxacin 75 mins 88%			3	Yashas et al., 2021
PVDF-PB-GO membrane	137Cs 79.6%	NH ₄ Cl HNO ₃		5	Zhang et al., (2022a)
RGO/WO ₃	Sr ²⁺ 100%	HCl, HNO ₃ , H ₂ SO ₄		5	Mu et al., (2022)

CedopedCo34/RGO*	Tetracycline 10 mins 90%			3	Pervaiz et al., (2022)
MGO@PANI	CIP 30 min 97%	Methanol 80 °C 2hrs	94.5 % 75 %	5 10	Nodeh et al., (2018)
LDH/GO*	Gatifloxacin 60mins 98%	-		4	Deng et al., (2021)
Nitrogen-doped reduced graphene oxide beads (NrGOB) *	hydroxybenzoic acid 90 mins 100%	Peroxy monosulfate (PMS) solution for 1 h followed by ultrapure water		3	Hirani et al., (2022)
Graphene oxide nanosheet (GOS)	Sulfamethoxazole 110mins 122mgg ⁻¹				Rostamian and Behnejad (2016)
Magnetic Graphene Oxide (nGO)	Clonazepam 180mins 14.41mgg ⁻¹	HCl	90 %	5	Nascimento et al., (2022)

1172 *catalytic degradation;

1173

1174 9. Future Perspectives

1175 The potential of graphene and its composites in wastewater treatment application towards the
1176 removal of biomedical pollutants and toxic compounds is significant. Novel treatment methods
1177 were developed years ago and their performance can be improved by incorporating novel
1178 functional materials like GO and graphene-based nanoparticles. Simultaneous adsorption and
1179 photodegradation is now seen as a new strategy in biomedical wastewater treatment beyond phase
1180 transfer offering degradation and possible mineralization of pollutants. Studying the influential
1181 factors and underlying mechanism that accompany the treatment process will also go a long way
1182 to improve the understanding and subsequent applicability of these materials. Researchers are also
1183 beginning to introduce graphene and its derivatives into traditional photocatalyst like ZnO and
1184 TiO₂. The success of this hybrid nanoparticle has been validated by recent research which positions
1185 it as one of the most promising technologies in wastewater decontamination and treatment (Nazal
1186 et al., 2020; Gao et al., 2020; Zheng et al., 2020). However, the treatment efficacy for real
1187 biomedical waste considering the presence of multiple contaminants is yet unknown and should
1188 be further looked into. Little work relating to process optimization methods such as Taguchi and
1189 response surface methodology have been carried out. Research on optimal conditions that ensure

1190 maximum treatment efficiency is encouraged if full scale deployment and industrial application is
1191 going to be achieved. Life cycle assessment studies that map out raw material acquisition,
1192 synthesis, use, and disposal are encouraged to reduce its environmental impact and ensure
1193 sustainability.

1194

1195 **10. Conclusion**

1196 The benefits of medicine and medical healthcare are undisputed; however, production and
1197 extensive use has resulted in waste generation and biomedical pollution. With current innovation,
1198 development and advanced medical technology, there are new challenges such as biomedical waste
1199 management. For instance, the amount of waste generated during production of pharmaceuticals
1200 varies greatly in amount and type (~200 to 30,000 kg of wastes per kg of active ingredients can be
1201 generated), relatively higher than the actual finished product. Existing treatment methods cannot
1202 meet quality threshold values regulations while government authorities impose stricter measures.
1203 Medical facilities are thus faced with challenges associated with adequate treatment of the waste
1204 and effluents they generate. More advanced technologies have been sought as conventional
1205 methods can no longer handle emerging contaminants vis-à-vis the stricter regulatory guidelines.
1206 High surface area, improved chemical properties, lower cost, and high regeneration capacity for
1207 reuse make nanomaterials advantageous for treatment processes in wastewater management and
1208 decontamination. Graphene and graphene oxide (GO) are a unique nanomaterial for water and
1209 wastewater treatment. They possess inherent chemical and physicochemical properties such as
1210 good biocompatibility, high surface area, optical, thermal and electrical conductivities, making
1211 them unique and very suitable for decontaminating wastewater. Nevertheless, little has been
1212 extensive research for possibility of its application in biomedical waste treatment except for
1213 antibiotics and related metabolites.

1214

1215

1216

1217

1218

1219

1220

1221 **Acknowledgement**

1222 The authors acknowledge the Ministry of Higher Education (MOHE), Malaysia for providing the
1223 research funding under project code FRGS/1/2019/TK10/CURTIN/02/2. We also thank Curtin
1224 University Malaysia for providing research facility and financial support for the project.

1225

1226 **Funding**

1227 Fundamental Research Grant Scheme (FRGS) under project code
1228 FRGS/1/2019/TK10/CURTIN/02/2

1229

1230 **Author Contributions**

1231 Kehinde Shola Obayomi: Conceptualization, Methodology, Writing Original draft preparation. Sie
1232 Yon Lau: Supervision, Validation, Resources. Ibitogbe Enoch Mayowa: Writing, Reviewing and
1233 Editing. Michael K. Danquah: Writing, Reviewing and Editing. Jianhua Zhang: Writing,
1234 Reviewing and Editing. Tung Chiong: Writing, Reviewing and Editing. Takeo Masahiro: Writing,
1235 Reviewing and Editing.

1236

1237 **References**

- 1238 Acheson, E. G., 1896. Manufacture of Graphite. US patent 568323. 1896.
- 1239 Ahmad, S. Z. N., Salleh, W. N. W., Ismail, A. F., Yusof, N., Yusop, M. Z. M., Aziz, F., 2020.
1240 Adsorptive removal of heavy metal ions using graphene-based nanomaterials: Toxicity,
1241 roles of functional groups and mechanisms, *Chemosphere*, 248, 126008.
- 1242 Aghamohammadi, H., Eslami-Farsani, R., Torabian, M., Amousa, N., 2020. Recent advances in
1243 one pot functionalization of graphene using electrochemical exfoliation of graphite: a
1244 review study, *Synthetic Metals*, 269, 116549.
- 1245 Agrawal, P., Kaur, G., Kolekar, S. S., 2021. Investigation on biomedical waste management of
1246 hospitals using cohort intelligence algorithm, *Soft Computing Letters*, 3, 100008.
- 1247 Ahmed, M. B., Zhou, J. L., Ngo, H. H., Guo, W., Thomaidis, N. S., Xu, J., 2017. Progress in the
1248 biological and chemical treatment technologies for emerging contaminant removal from
1249 wastewater: a critical review. *Journal of hazardous materials*, 323, 274-298.
- 1250 Ajala, O. J., Tijani, J. O., Bankole, M. T., Abdulkareem, A. S., 2022. A critical review on
1251 graphene oxide nanostructured material: Properties, Synthesis, characterization and
1252 application in water and wastewater treatment, *Environmental Nanotechnology, Monitoring
1253 and Management*, 18, 100673.
- 1254 Alamgholiloo, H., Pesyan, N. N., Mohammadi, R., Rostannia, S., Shokouhimehr, M. 2021.
1255 Synergistic advanced oxidation process for the fast degradation of ciprofloxacin antibiotics

1256 using a GO/CuMOF-magnetic ternary nanocomposite. *Journal of Environmental Chemical*
1257 *Engineering*, 9(4), 105486.

1258 Ali, I., Basheer, A. A., Mbianda, X. Y., Burakov, A., Galunin, E., Burakova, I., Mkrtychyan, E.,
1259 Tkachev, A., Grachev, V., 2019. Graphene based adsorbents for remediation of noxious
1260 pollutants from wastewater, *Environmental International*, 127, 160-180.

1261 Ali, A., Shoeb, M., Li, Y., Li, B., Khan, M. A., 2021. Enhanced photocatalytic degradation of
1262 antibiotic drug and dye pollutants by graphene-ordered mesoporous silica (SBA 15)/TiO₂
1263 nanocomposite under visible-light irradiation *Journal of Molecular Liquids*, 324, 114696.

1264 Ali, A., Shoeb, M., Li, B., Khan, M. A., 2022. Photocatalytic degradation of antibiotic drug and
1265 dye pollutants under visible-light irradiation by reduced graphene oxide decorated
1266 MoO₃/TiO₂ nanocomposite, *Materials Science in Semiconductor Processing*, 150, 106974.

1267 AL-Othman, Z. A., AlMasoud, N., Mbianda, X. Y., Ali, I., 2022. Synthesis and characterization
1268 of γ -cyclodextrin-graphene oxide nanocomposite: Sorption, kinetics, thermodynamics and
1269 simulation studies of tetracycline and chlortetracycline antibiotics removal in water,
1270 *Journal of Molecular Liquids*, 345, 116993.

1271 Al-Jubouri, S. M., Al-Jendeel, H. A., Rashid, S. A., Al-Batty, S., 2022. Antibiotics adsorption
1272 from contaminated water by composites of ZSM-5 zeolite nanocrystals coated carbon, *Journal*
1273 *of Water Process Engineering*, 47, 2022, 102745.

1274 Al-Khateeb, L. A., Almotiry, S., Salam, M. A., 2014. Adsorption of pharmaceutical pollutants
1275 onto graphene nanoplatelets, *Chemical Engineering Journal*, 248, 191-199.

1276 ALothman, Z. A., AlMasoud, N., Mbianda, X. Y., Ali, I., 2022. Synthesis and characterization of
1277 γ -cyclodextrin-graphene oxide nanocomposite: Sorption, kinetics, thermodynamics and
1278 simulation studies of tetracycline and chlortetracycline antibiotics removal in water, *Journal*
1279 *of Molecular Liquids*, 345, 116993.

1280 Alshamkhani, M. T., Teong, L. K., Putri, L. K., Mohamed, A. R., Lahijani, P., Mohammadi, M.,
1281 2021. Effect of graphite exfoliation routes on the properties of exfoliated graphene and its
1282 photocatalytic applications, *Journal of Environmental Chemical Engineering* 9, 106506.

1283 Amine, A. E. K. 2013. Extended spectrum beta-lactamase producing bacteria in waste water
1284 alexandria, Egypt. *International Journal of Bioscience, Biochemistry and*
1285 *Bioinformatics*, 3(6), 605.

1286 Amiria, A., Naraghib, M., Ahmadi, G., Soleymanihaa, M., Shanbedid, M., 2018. A review on
1287 liquid-phase exfoliation for scalable production of pure graphene, wrinkled, crumpled and
1288 functionalized graphene and challenges, *FlatChem*, 8, 40-71.

1289 Andrade, M. B., Santos, T. R. T., Guerra, A. C. S., Silva, M. F., Demiti, G. M. M., Bergamasco,
1290 R., 2022. Evaluation of magnetic nano adsorbent produced from graphene oxide with iron
1291 and cobalt nanoparticles for caffeine removal from aqueous medium, *Chemical*
1292 *Engineering and Processing - Process Intensification*, 170, 108694.

1293 Anirudhan, T.S., Deepa, J.R., Nair, A.S., 2017a. Fabrication of chemically modified graphene
1294 oxide/nano hydroxyapatite composite for adsorption and subsequent photocatalytic
1295 degradation of aureomycine hydrochloride. *Journal of Industrial and Engineering*
1296 *Chemistry*, 47, 415-430.

1297 Anuma, S., Mishra, P., Bhat, B. R., 2021. Polypyrrole functionalized Cobalt oxide Graphene
1298 (COPYGO) nanocomposite for the efficient removal of dyes and heavy metal pollutants
1299 from aqueous effluents *Journal of Hazardous Materials*, 416, 125929.

1300 Ara, L., Billah, W., Bashar, F., Mahmud, S., Amin, A., Iqbal, R., Rahman, T., Alam, N. H., Sarker,
1301 S. A., 2022. Effectiveness of a multi-modal capacity-building initiative for upgrading
1302 biomedical waste management practices at healthcare facilities in Bangladesh: a 21st century
1303 challenge for developing countries, *Journal of Hospital Infection*, 121, 49-56

1304 Assouik, J., Hajji, L., Boukir, A., Herold, C., Lagrange, P., 2016. Synthesis, structure, and
1305 electrical behavior of the heavy alkali metal-arsenic alloys-based graphite intercalation
1306 compounds, *Synthetic Metals*, 218, 34-42.

1307 Aunkor, M. T. H., Mahbulul, I. M., Saidur, R., Metselaar, H. S. C. 2016. The green reduction of
1308 graphene oxide, *RSC Advances*, 6 (33), 27807–27828.

1309 Awad, A. M., Jalab, R., Benamor, A., Nasser, M. S., Ba-Abbad, M. M., El-Naas, M., Mohammad,
1310 A., 2020. Adsorption of organic pollutants by nanomaterial-based adsorbents: An overview,
1311 *Journal of Molecular Liquids*, 301, 112335.

1312 Baig, N., Sajid, M., Saleh, T. A. 2019. Graphene-based adsorbents for the removal of toxic organic
1313 pollutants: A review. *Journal of environmental management*, 244, 370-382.

1314 Balasubramani, K., Sivarajasekar, N., Naushad, M., Effective adsorption of antidiabetic
1315 pharmaceutical (metformin) from aqueous medium using graphene oxide nanoparticles:
1316 Equilibrium and statistical modelling, 2020. *Journal of Molecular Liquids*, 301, 1 March
1317 2020, 112426.

1318 Basagni, A., Sedona, F., Pignedoli, C. A., Cattelan, M., Nicolas, L., Casarin, M., Sambri, M., 2015.
1319 Molecules–Oligomers–Nanowires–Graphene Nanoribbons: A Bottom-Up Stepwise On-
1320 Surface Covalent Synthesis Preserving Long-Range Order, *Journal of Physical Chemistry C*,
1321 137, 5.

1322 Baumgarten, S., Schröder, H. F., Charwath, C., Lange, M., Beier, S., Pinnekamp, J., 2007.
1323 Evaluation of advanced treatment technologies for the elimination of pharmaceutical
1324 compounds. *Water science and technology*, 56(5), 1-8.

1325 Bharath, G., Alhseinat, E., Ponpandian, N., Khan, M. A., Siddiqui, M. R., Ahmed, F., Alsharaeh,
1326 E. H., 2017. Development of adsorption and electrosorption techniques for removal of organic
1327 and inorganic pollutants from wastewater using novel magnetite/porous graphene-based
1328 nanocomposites, *Separation and Purification Technology*, 188, 206-218.

1329 Bhuyan, M, S, A., Uddin, M. N., Islam, M. M., Bipasha, F. A., Hossain, S. S., 2016. Synthesis of
1330 graphene, *International Nano Letters*, 6, 65.

1331 Biswal, S. (2013). Liquid biomedical waste management: An emerging concern for
1332 physicians. *Muller Journal of Medical Sciences and Research*, 4(2), 99.

1333 Bo, Z., Shuai, X., Mao, S., Yang, H., Qian, J., Chen, J., 2014. Green preparation of reduced
1334 graphene oxide for sensing and energy storage applications, *Scientific Report*. 4, 4684.

1335 Brodie, B.C., 1859. On the atomic weight of graphite. *Philos. Trans. Roy. Soc. Lond.*149, 249-
1336 259.

1337 Bouhafs, C., Pezzini, S., Geisenhof, R. F., Mishra, N., Mišeikis, V., Niu, Y., Struzzi, C., Weitz, R.
1338 T., Forti, S., Coletti, C., 2022. Synthesis of large-area rhombohedral few-layer graphene by
1339 chemical vapor deposition on copper, *Carbon*, 177, 282-290.

1340 Bulin, C., Zhang, Y., Li, B., Zhang, B. 2020. Removal performance of aqueous Co (II) by magnetic
1341 graphene oxide and adsorption mechanism. *Journal of Physics and Chemistry of Solids*, 144,
1342 109483.

- 1343 Cao, M., Wang, P., Ao, Y., Wang, C., Hou, J., Qian, J., 2016. Visible light activated photocatalytic
1344 degradation of tetracycline by a magnetically separable composite photocatalyst: Graphene
1345 oxide/magnetite/cerium-doped titania, *Journal of Colloid and Interface Science*, 467, 129-139.
- 1346 Carballa, M. Omil, F. and Lema, J. M., 2008. Comparison of predicted and measured
1347 concentrations of selected pharmaceuticals, fragrances and hormones in Spanish sewage,
1348 *Chemosphere*, 72: 1118–1123
- 1349 Chao, Y., Tang, B., Luo, J., Wu, P., Tao, D., Chang, H., Chu, X., Huang, Y., Li, H., Zhu, W. 2021.
1350 Hierarchical porous boron nitride with boron vacancies for improved adsorption performance
1351 to antibiotics, *Journal of Colloid Interface Science*, 584, 154-163.
- 1352 Chartier, Yves, ed. Safe management of wastes from health-care activities. World Health
1353 Organization, 2014.
- 1354 Chen, J., Yao, B., Li, C., Shi, G., 2013. An improved Hummers method for eco-friendly synthesis
1355 of graphene oxide, *Carbon*, 64, 225-229.
- 1356 Chen, F., Yang, Q., Li, X., Zeng, G., Wang, D., Niu, C., Zhao, J., An, H., Xie, T., Deng, Y., 2017.
1357 Hierarchical assembly of graphene-bridged $\text{Ag}_3\text{PO}_4/\text{Ag}/\text{BiVO}_4$ (040) Zscheme photocatalyst:
1358 an efficient, sustainable and heterogeneous catalyst with enhanced visible-light photoactivity
1359 towards tetracycline degradation under visible light irradiation, *Applied Catalysis B:
1360 Environmental*, 200, 330-342.
- 1361 Chen, F., Liang, W., Qin, X., Jiang, L., Zhang, Y., Fang, S., Luo, D., 2021. Preparation and
1362 recycled simultaneous adsorption of methylene blue and Cu^{2+} co-pollutants over carbon layer
1363 encapsulated Fe_3O_4 /graphene oxide nanocomposites rich in amino and thiol groups, *Colloids
1364 and Surfaces A: Physicochemical and Engineering Aspects*, 625, 126913.
- 1365 Choi, W., Lahiri, I., Seelaboyina, R., Kang, Y. S., 2010. Synthesis of graphene and its applications:
1366 a review, *Critical Review in Solid State* 35 (1), 52–71.
- 1367 Choucair, M., Thordarson, P., Stride, J. A., 2009. Gram-scale production of graphene based on
1368 solvo thermal synthesis and sonication, *Nature Nanotechnology*, 4 (1), 30–33.
- 1369 Ciesielski, A., Samorì, P., 2014. Graphene via sonication assisted liquid-phase exfoliation,
1370 *Chemical Society Reviews* 43 (1), 381–398.
- 1371 Compton, O. C., An, Z., Putz, K. W., Hong, B. J., Hauser, B. G., Brinson, L. C., Nguyen, S. T.,
1372 2012. Additive-free hydrogelation of graphene oxide by ultrasonication, *Carbon*, 50 (10),
1373 3399-3406.
- 1374 Coraux, J., N'Diaye, A. T., Busse, C., Michely, T., 2008. Structural coherency of graphene on
1375 Ir(111), *Nano Letters*, 8 (2), 565–570.
- 1376 Crini, G., and Lichtfouse, E., 2019. Advantages and disadvantages of techniques used for
1377 wastewater treatment. *Environmental Chemistry Letters*, 17, 1, 145-155.
- 1378 Das, R., Talat, M., Srivastava, O. N., Kayastha, A. M., 2018. Covalent immobilization of peanut
1379 β -amylase for producing industrial nanobiocatalysts: A comparative study of kinetics, stability
1380 and reusability of the immobilized enzyme, *Food Chemistry*, 245, 488-499.
- 1381 Dash, K., Das, M., Satapathy, N. K., 2021. Assessment of knowledge, attitude, and practices about
1382 biomedical waste management among nursing professionals in a Tertiary Care Hospital,
1383 Bhubaneswar, Odisha, *European Journal of Molecular & Clinical Medicine*, 8 (3), 1127-1142.

1384 Deng, J., Xiao, L., Yuan, S., Wang, W., Zhan, X. and Hu, Z.H., 2021. Activation of
1385 peroxymonosulfate by CoFeNi layered double hydroxide/graphene oxide (LDH/GO) for the
1386 degradation of gatifloxacin. *Separation and Purification Technology*, 255, 117685.

1387 Dulama, M., Deneanu, N., Dulama, C., Pavelescu, M. 2008. Experimental studies concerning the
1388 semipermeable membrane separation efficiency for Cs-134, Cs-137, Co-57, Co-58, Co-60,
1389 Mn-54 in liquid radioactive waste. *Rev Chim*, 59, 544-549.

1390 Ebratkhahan, M., Zarei, M., Akpınar, I. Z., Metin, O., 2022. One-pot synthesis of graphene
1391 hydrogel/M (M: Cu, Co, Ni) nanocomposites as cathodes for electrochemical removal of
1392 rifampicin from polluted water, *Environmental Research*, 214, 113789.

1393 Elmolla, E. S., Chaudhuri, M., 2010. Photocatalytic degradation of amoxicillin, ampicillin and
1394 cloxacillin antibiotics in aqueous solution using UV/TiO₂ and UV/H₂O₂/TiO₂ photocatalysis,
1395 *Desalination*, 252, (1–3), 46-52.

1396 Ersan, G., Apul, O. G., Perreault, F., Karanfil, T., 2017. Adsorption of organic contaminants by
1397 graphene nanosheets: A review, *Water Research*, (126), 385-398.

1398 Fakhri, H., Bagheri, H., 2020. Highly efficient Zr-MOF@WO₃/graphene oxide photocatalyst:
1399 Synthesis, characterization and photodegradation of tetracycline and malathion, *Materials*
1400 *Science in Semiconductor Processing*, 107, 104815.

1401 Fang, M., Wang, K., Lu, H., Yang, Y., Nutt, S., 2009. Covalent polymer functionalization of
1402 graphene nanosheets and mechanical properties of composites, *Journal of Materials*
1403 *Chemistry*, 19 (38), 7098–7105.

1404 Feng, J-B., Li, Y-Y., Zhang, Y., Xu, Y-Y., Cheng, X-W., 2022. Adsorptive removal of
1405 indomethacin and diclofenac from water by polypyrrole doped-GO/COF-300
1406 nanocomposites, *Chemical Engineering Journal*, 429, 132499.

1407 Figueiredo, B. R., Cardoso, S. P., Portugal, I., Rocha, J., Silva, C. M. (2018). Inorganic ion
1408 exchangers for cesium removal from radioactive wastewater. *Separation and Purification*
1409 *Reviews*, 47(4), 306-336.

1410 Freundlich, H. M. F., 1906. Over the adsorption in solution, *Journal of Physical Chemistry*, 57,
1411 385–471.

1412 Gadipelly, C., Pérez-González, A., Yadav, G.D., Ortiz, I., Ibáñez, R., Rathod, V.K. Marathe, K.V.,
1413 2014. Pharmaceutical industry wastewater: review of the technologies for water treatment and
1414 reuse. *Industrial & Engineering Chemistry Research*, 53, 29, 11571-11592.

1415 Gao, Y., Li, Y., Zhang, L., Huang, H., Hu, J., Shah, S. M., Su, X. 2012. Adsorption and removal
1416 of tetracycline antibiotics from aqueous solution by graphene oxide. *Journal of colloid and*
1417 *interface science*, 368(1), 540-546.

1418 Gao, E., Lin, S.-Z., Qin, Z., Buehler, M. J., Feng, X.-Q., Xu, Z., 2018. Mechanical exfoliation of
1419 two-dimensional materials, *Journal of Mechanics, and Physics of Solids*, 115, 248-262.

1420 Gao, Z., Wang, S., Berry, J., Zhang, Q., Gebhardt, J., Parkin, W. M., Avila, J., Yi, H., Chen, C.,
1421 Hurtado-Parra, S., Drndić, M., Rappe, A. M., Srolovitz, D. J., Kikkawa, J. M., Luo, Z.,
1422 Asensio, M. C., Wang, F., Johnson, A. T. C., 2020. Large-area epitaxial growth of curvature-
1423 stabilized ABC trilayer graphene, *Nature Communications*, 11, 546,

1424 Ghorbanih, M., Salem, S., 2021. Removal of chemical oxygen demand from industrial estate
1425 sewage over hybridized anatase-graphene oxide-carbon nanotubes nanocomposite under solar
1426 irradiation, *Process Safety and Environmental Protection*, 149, 581-590.

1427 Grisales-Cifuentes, C. M., Galvis, E. A. S., Porras, J., Flórez, E., Torres-Palma, R. A., Acelas, N.,
1428 2021. Kinetics, isotherms, effect of structure, and computational analysis during the removal
1429 of three representative pharmaceuticals from water by adsorption using a biochar obtained
1430 from oil palm fiber, *Bioresource Technology*, 326, 124753.

1431 Guan, Z., Li, X., Wu, Y. Chen, Z., Huang, X, Wang, D., Yang, Q., Liu, J., Tian, S., Chen, X.,
1432 Zhao, H., 2021. AgBr nanoparticles decorated 2D/2D GO/Bi₂WO₆ photocatalyst with
1433 enhanced photocatalytic performance for the removal of tetracycline hydrochloride, *Chemical*
1434 *Engineering Journal*, 410, 128283.

1435 Guo, W., Cheng, D., Ngo, H. H., Chang, S. W., Nguyen, D. D., Nguyen, D. P., Bui, X. T. 2020.
1436 Anaerobic membrane bioreactors for antibiotic wastewater treatment. In *Current*
1437 *Developments in Biotechnology and Bioengineering*, 219-239.

1438 Haiba, E., Lillenberg, M., Kipper, K., Herodes, K. (2013). Degradation of some pharmaceuticals
1439 during sewage sludge composting. *Global Journal on Advances Pure and Applied Sciences*, 1.

1440 Han, Z., Xiao, X., Qu, H., Hu, M., Au, C., Nashalian, A., Xiao, X., Wang, Y., Yang, L., Jia, F.,
1441 Wang, T., Ye, Z., Servati, P., Huang, L., Zhu, Z., Tang, J., Chen, J., 2022. Ultrafast and
1442 Selective Nanofiltration Enabled by Graphene Oxide Membranes with Unzipped Carbon
1443 Nanotube Networks, *ACS Applied Materials and Interfaces*, 14(1),1850–1860.

1444 Hernandez, Y., Lotya, M., Rickard, D., Bergin, S. D., Coleman, J. N., 2010. Measurement of
1445 multicomponent solubility parameters for graphene facilitates solvent discovery, *Langmuir* 26
1446 (5) 3208–3213.

1447 Hernandez, Y., Nicolosi, V., Lotya, M., Blighe, F. M., Sun, Z., De, S., et al., 2008. High-yield
1448 production of graphene by liquid-phase exfoliation of graphite, *Nature Nanotechnology*, 3,
1449 563–568.

1450 Hiew, B. Y. Z., Lee, L. Y., Lee, X. J., Gan, S., Thangalazhy-Gopakumar, S., Lim, S. S., Pan, G-
1451 T., Yang, T. C-K., 2019. Adsorptive removal of diclofenac by graphene oxide:
1452 Optimization, equilibrium, kinetic and thermodynamic studies, *Journal of the Taiwan*
1453 *Institute of Chemical Engineers*, 98, 150-162.

1454 Hirani, R.A.K., Asif, A.H., Rafique, N., Wu, H., Shi, L., Zhang, S., Duan, X., Wang, S., Saunders,
1455 M. and Sun, H., 2022. Three-dimensional nitrogen-doped graphene oxide beads for catalytic
1456 degradation of aqueous pollutants, *Chemical Engineering Journal*, 446(2), 137042.

1457 Ho, Y. S., McKay, S., 1999. Pseudo-second order model for sorption processes, *Process*
1458 *Biochemistry*, 34, 451–465.

1459 Homem, V., Santos, L., 2011. Degradation and removal methods of antibiotics from aqueous
1460 matrices-a review, *Journal of Environmental Management.*, 92, 2304-2347

1461 Hooshmand, S., Kargozar, S., Ghorbani, A., Darroudi, M., Keshavarz, M., Baine, F., Kim, H. W.
1462 2020. Biomedical waste management by using nanophotocatalysts: The need for new
1463 options. *Materials*, 13(16), 3511.

1464 Hossain, M. F., Akther, N., Zhou, Y., 2020. Recent advancements in graphene adsorbents for
1465 wastewater treatment: Current status and challenges, *Chinese Chemical Letters*, 3110, 2525-
1466 2538.

1467 Hosseini, H., Zirakjou, A., McClements, D. J., Goodarzi, V., Chen, W-H., 2022. Removal of
1468 methylene blue from wastewater using ternary nanocomposite aerogel systems:
1469 Carboxymethyl cellulose grafted by polyacrylic acid and decorated with graphene oxide,
1470 *Journal of Hazardous Materials*, 421, 126752.

1471 Hsieh, M-L., Juang, R-S., Gandomi, Y-A., Fu, C-C., Hsieh, C-T., Liu, W-R., 2022. Synthesis and
1472 characterization of high-performance ZnO/graphene quantum dot composites for
1473 photocatalytic degradation of metronidazole, *Journal of the Taiwan Institute of Chemical*
1474 *Engineers*, 131, 104180.

1475 Hummers, W. S., Offeman, R. E., 1958. Preparation of graphitic oxide, *J. Am. Chem. Soc.* 80
1476 1339.

1477 Huang, B., Wang, H. C., Cui, D., Zhang, B., Chen, Z. B., & Wang, A. J. 2018. Treatment of
1478 pharmaceutical wastewater containing β -lactams antibiotics by a pilot-scale anaerobic
1479 membrane bioreactor (AnMBR). *Chemical Engineering Journal*, 341, 238-247.

1480 Huo, P., Zhou, M., Tang, Y., Liu, X., Ma, C., Yu, L., Yan, Y., 2016. Incorporation of NZnO/
1481 CdS/Graphene oxide composite photocatalyst for enhanced photocatalytic activity under
1482 visible light, *Journal of Alloys and Compounds*, 670, 198-209.

1483 Ikram, R., Jan, B. M., Ahmad, W., 2020. Advances in synthesis of graphene derivatives using
1484 industrial wastes precursors; prospects and challenges, *Journal of Materials Research and*
1485 *Technology*, 9, (6), 15924-15951.

1486 Innemanová, P., Grasserová, A., Cajthaml, T. 2022. Pilot-scale vermicomposting of dewatered
1487 sewage sludge from medium-sized wwtp. *detritus*, 18, 35.

1488 International Atomic Energy Agency. (2000). Management of radioactive waste from the use of
1489 radionuclides in medicine. International Atomic Energy Agency.

1490 Iqbal, A. A., Sakib, N., Iqbal, A. K. M. P., Nuruzzaman, D. M., 2020. Graphene-based
1491 nanocomposites and their fabrication, mechanical properties, and applications, *Materialia*, 12,
1492 100815.

1493 Januário, E. F. D., Fachina, Y. J., Wernke, G., Demiti, G. M. M., Beltran, L. B., Bergamasco, R.,
1494 Vieira, A. M. S., 2022. Application of activated carbon functionalized with graphene oxide
1495 for efficient removal of COVID-19 treatment-related pharmaceuticals from water,
1496 *Chemosphere*, Volume 289, 133213.

1497 Jaswal, A., Kaur, M., Singh, S., Kansal, S. K., Umar, A., Garoufalidis, C. S., Baskoutas, S.,
1498 Adsorptive removal of antibiotic ofloxacin in aqueous phase using rGO-MoS₂ heterostructure,
1499 2021. *Journal of Hazardous Materials*, 417, 125982.

1500 Jeyaseelan, A., Ghfar, A. A., Naushad, M, Viswanathan, 2021. Design and synthesis of amine
1501 functionalized graphene oxide for enhanced fluoride removal *Journal of Environmental*
1502 *Chemical Engineering*, 9 (4), 105384.

1503 Jia, F., Xiao, X., Nashalian, A., Shen, S., Yang, L., Han, Z., Qu, H., Wang, T., Ye, Z., Zhu,
1504 Z., Huang, L., Wang, Y., Tang, J., Chen, J., 2022. Advances in graphene oxide
1505 membranes for water treatment, *Nano Research*, 15, 6636–6654.

1506 Juengchareonpon, K., Wanichpongpan, P., Boonamnuyvitaya, B., 2021. Graphene oxide and
1507 carboxymethylcellulose film modified by citric acid for antibiotic removal, *Journal of*
1508 *Environmental Chemical Engineering*, 9(1), 104637.

1509 Julkapli, N.M., Bagheri, S., 2015. Graphene supported heterogeneous catalysts: an overview,
1510 *International Journal of Hydrogen Energy*, 40, 948-979.

1511 Kedves, A., Rónavári, A., Kónya, Z., 2021. Long-term effect of graphene oxide on the aerobic
1512 granular sludge wastewater treatment process, *Journal of Environmental Chemical*
1513 *Engineering*, 9(1), 104853.

1514 Khan, S., Syed, A. T., Ahmad, R., Rather, T. A., Ajaz, M., & Jan, F. A. 2010. Radioactive waste
1515 management in a hospital. *International journal of health sciences*, 4(1), 39.

1516 Khanday, W. A., Ahmed, M. J., Okoye, P. U., Hummadi, E. H., Hameed, B. H., 2019. Single-step
1517 pyrolysis of phosphoric acid-activated chitin for efficient adsorption of cephalexin antibiotic,
1518 *Bioresource Technology*, 280, 255-259.

1519 Kim, S., Marion, M., Jeong, B.H., Hoek, E.M.V., 2006. Crossflow membrane filtration of
1520 interacting nanoparticle suspensions. *Journal of Membrane Science*, 284, 361–372.

1521 Kim, K. S., Zhao, Y., Jang, H., Lee, S. Y., Kim, J. M., Kim, K. S., Ahn, J-H., Kim, P., Choi, J-Y.,
1522 Hong, B. H., 2009. Large-scale pattern growth of graphene films for stretchable transparent
1523 electrodes, *Nature*, 457, 706–710.

1524 Komal, Gupta, K., Nidhi Kaushik, A., Singhal, S., 2022. Amelioration of adsorptive efficacy by
1525 synergistic assemblage of functionalized graphene oxide with esterified cellulose nanofibers
1526 for mitigation of pharmaceutical waste, *Journal of Hazardous Materials*, 424, Part B, 127541.

1527 Kovtyukhova, N. I., Ollivier, P. J., Martin, B. R., Mallouk, T. E., Chizhik, S. A., Buzaneva, E. V.,
1528 1999. Layer-by-Layer assembly of ultrathin composite films from micron-sized graphite
1529 oxide sheets and polycations, *Chemistry of Materials*, 11 (3), 771–778.

1530 Kumar, N., Salehiyan, R., Chauke, V., Botlhoko, O. J., Setshedi, K., Scriba, M., Masukume, M.,
1531 Ray, S. S., 2021. Top-down synthesis of graphene: A comprehensive review, *FlatChem*, 27,
1532 100224.

1533 Kumari, T. S. D., 2021. Catalytic graphitization: A bottom-up approach to graphene and quantum
1534 dots derived therefrom – A review, *Materialstoday: Proceedings*, 46(8), 3069-3074.

1535 Kyzas, G. Z., Deliyanni, E. A., Bikiaris, D. N., Mitropoulos, A. C., 2018. Graphene composites as
1536 dye adsorbents: Review, *Chemical Engineering Research and Design*, 129, 75–88.

1537 Lagergren, S., Svenska, B. K., 1898. On the theory of so-called adsorption of dissolved substances,
1538 *The Royal Swedish Academy of Sciences Document*, Band 24, 1–13.

1539 Langmuir, I., 1916. The constitution and fundamental properties of solids and liquids, *Journal of*
1540 *the American Chemical Society*, 38 (11), 2221-2295.

1541 Lee, L., Noh, S., Pham, N. D., Shim, J. H., 2019. Top-down synthesis of S-doped graphene
1542 nanosheets by electrochemical exfoliation of graphite: metal-free bifunctional catalysts for
1543 oxygen reduction and evolution reactions, *Electrochim. Acta*, 313, 1-9.

1544 Lefebvre, O., Shi, X., Wu, C. H., Ng, H. Y. (2014). Biological treatment of pharmaceutical
1545 wastewater from the antibiotics industry. *Water science and technology*, 69(4), 855-861.

1546 Lehto, J., Koivula, R., Leinonen, H., Tusa, E., Harjula, R. (2019). Removal of radionuclides from
1547 Fukushima Daiichi waste effluents. *Separation & Purification Reviews*, 48(2), 122-142.

1548 Letcher, T. M., Slack, R. (2019, January). *Chemicals in Waste: Household Hazardous Waste*.
1549 In *Waste* (pp. 337-352). Academic Press.

1550 Li, N., Wang, Z., Zhao, K., Shi, Z., Gu, Z., Xu, S., 2009. Large scale synthesis of N-doped multi-
1551 layered graphene sheets by simple arc-discharge method, *Carbon* 48 (1), 255–259.

1552 Li, M-F., Liu, Y-G., Zeng, G-M., Liu, N., Liu, S-B., 2019. Graphene and graphene-based
1553 nanocomposites used for antibiotics removal in water treatment: A review, *Chemosphere* 226,
1554 360-380.

1555 Li, F-M., Liu, Y-G, Zeng, G-M., Liu, N., Liu, S-B., 2019. Graphene and graphene-based
1556 nanocomposites used for antibiotics removal in water treatment: A review, *Chemosphere* 226,
1557 360380.

1558 Li, y., Lai, Z., Huang, Z., Wang, H., Zhao, C., Ruan, G., Du, F., 2021. Fabrication of
1559 BiOBr/MoS₂/graphene oxide composites for efficient adsorption and photocatalytic removal
1560 of tetracycline antibiotics, *Applied Surface Science*, 550, 149342.

1561 Lim, J. Y., Mubarak, N. M., Abdullah, E. C., Nizamuddin, S., Khalid, M., Inamuddin, 2018.
1562 Recent trends in the synthesis of graphene and graphene oxide- based nanomaterials for
1563 removal of heavy metals — A review, *Journal of Industrial and Engineering Chemistry* 66,
1564 29–44.

1565 Lin, T., Tang, Y., Wang, Y., Bi, H., Liu, Z., Huang, F., Xie, X., Jiang, M., 2013. Scotch-tape-like
1566 exfoliation of graphite assisted with elemental sulfur and graphene–sulfur composites for
1567 high-performance lithium-sulfur batteries, *Energy and Environmental Science*, 6, 4, 1283-
1568 1290.

1569 Lin, Y., Xu, S., Li, J. 2013. Fast and highly efficient tetracyclines removal from environmental
1570 waters by graphene oxide functionalized magnetic particles. *Chemical Engineering*
1571 *Journal*, 225, 679-685.

1572 Lin, Z., Karthik, P. S., Hada, M., Nishikawa, T., Hayashi, Y., 2017. Simple technique of
1573 exfoliation and dispersion of multilayer graphene from natural graphite by ozone-assisted
1574 sonication, *Nanomaterials*, 7 (6), 125.

1575 Liu, J., Liu, L., Sun, D. D., 2012. Graphene oxide enwrapped Ag₃PO₄ composite: towards a highly
1576 efficient and stable visible-light-induced photocatalyst for water purification. *Catalysis*
1577 *Science and Technology*, 2, 2525-2532.

1578 Liu, J., Ruffieux, P., Feng, X., Müllen, K., Fasel, R., 2014. Cyclotrimerization of arylalkynes on
1579 Au(III), *Chemical Communications*, 50, 11200-11203.

1580 Ma, F., Li, Z., Zhao, H., Geng, Y., Zhou, W., Li, Q., Zhang, L., 2017. Potential application of
1581 graphene oxide membranes for removal of Cs(I) and Sr(II) from high level-liquid waste,
1582 *Separation and Purification Technology*, 188, 523-529.

1583 Ma, Z., Wu, H., Zhang, K., Xu, X., Wang, C., Zhu, W., & Wu, W. 2018. Long-term low dissolved
1584 oxygen accelerates the removal of antibiotics and antibiotic resistance genes in swine
1585 wastewater treatment. *Chemical Engineering Journal*, 334, 630-637.

1586 Ma, C., Yang, S., Cheng, Y., Xing, Z. 2020. Study on preparation of magnetic graphene oxide
1587 composites and its adsorption performance for Cr³⁺ in tannery wastewater. *Liaoning*
1588 *Chemical Industry*, 49(09), 1072–1074.

1589 Mohamed, K. A., Ahmed, E. S., Mohamed, A., Mohamed, M., El-Desoky, Senentxu, L. M., 2021.
1590 Silver-doped cadmium selenide/graphene oxide-filled cellulose acetate nanocomposites
1591 for photocatalytic degradation of malachite green toward wastewater treatment, *ACS*
1592 *Omega*, 6, 23129-23138.

1593 Mahmoodi, N. M., Oveisi, M., Bakhtiari, M., Hayati, B., Shekarchi, A. A., Bagheri, A., Rahimi,
1594 S., 2019. Environmentally friendly ultrasound-assisted synthesis of magnetic zeolitic
1595 imidazolate framework - Graphene oxide nanocomposites and pollutant removal from water,
1596 *Journal of Molecular Liquids*, 282, 115-130.

1597 Mohan, V. B., Liu, D., Jayaraman, K., Stamm, M., Bhattacharyya, D., 2016. Improvements in
1598 electronic structure and properties of graphene derivatives, *Advanced Materials Letter*, 7 (6),
1599 421–429.

1600 Moreira, V. R., Lebron, Y. A. R., da Silva, M. M., Santos, L. V., Jacob, R. S., de Vasconcelos,
1601 C. K. B., Viana, M. M., 2020. Graphene oxide in the remediation of norfloxacin from aqueous
1602 matrix: simultaneous adsorption and degradation process, *Environmental Science and*
1603 *Pollution Research*, 27, 34513–34528.

1604 Mortazavi, M., Baghdadi, M., Javadi, N. H. S., Torabian, A. 2019. The black beads produced by
1605 simultaneous thermal reducing and chemical bonding of graphene oxide on the surface of
1606 amino-functionalized sand particles: Application for PAHs removal from contaminated
1607 waters, *Journal of Water Process Engineering*, 31, 100798.

1608 Mu, W., Qianhong, Q., Hu, R., Li, X., Wei, H., Jian, Y. 2017. Porous three-dimensional reduced
1609 graphene oxide merged with WO₃ for efficient removal of radioactive strontium, *Applied*
1610 *Surface Science*, 423, 1203-1211.

1611 Muralikrishna, I. V., Manickam, V., 2017. Chapter One—Introduction. *Environmental*
1612 *Management*, 1-4.

1613 Nagarajan, L., Saravanan, P., Kumaraguru, K., Joo, S-W., Vasseghian, Y., Rajeshkannan, R.,
1614 Rajasimman, M. 2022. Synthesis of magnesium nanocomposites decked with multilayer
1615 graphene (MG) and its application for the adsorptive removal of pollutant *Chemosphere*, 298,
1616 134121.

1617 Nam, S.W., Jung, C., Li, H., Yu, M., Flora, J.R., Boateng, L.K., Her, N., Zoh, K.D., Yoon, Y.,
1618 2015. Adsorption characteristics of diclofenac and sulfamethoxazole to graphene oxide in
1619 aqueous solution. *Chemosphere*, 136, 20-26.

1620 Nayak, L., Rahaman, M., Moukwa, M., 2022 Synthesis/preparation and surface
1621 modification/functionalization of graphene, and concept of nanocomposites, *Polymer*
1622 *Nanocomposites Containing Graphene*, 1-44.

1623 Ninwiwek, N., Hongsawat, P., Punyapalukul, P., Prarat, P., 2019. Removal of the antibiotic
1624 sulfamethoxazole from environmental water by mesoporous silica-magnetic graphene oxide
1625 nanocomposite technology: Adsorption characteristics, coadsorption and uptake mechanism,
1626 *Colloids and Surfaces A: Physicochemical and Engineering Aspects*, 580 (5), 123716.

1627 Niu, L., Coleman, J. N., Zhang, H., Shin, H., Chhowalla, M., Zheng, Z., 2016. Production of two-
1628 dimensional nanomaterials via liquid-based direct exfoliation, *Small* 12 (3), 272–293.

1629 Nodeh, M. K. M., Soltani, S., Shahabuddin, S., Rashidi Nodeh, H., Sereshti, H. 2018. Equilibrium,
1630 kinetic and thermodynamic study of magnetic polyaniline/graphene oxide-based
1631 nanocomposites for ciprofloxacin removal from water. *Journal of Inorganic and*
1632 *Organometallic Polymers and Materials*, 28(3), 1226-1234.

1633 Novoselov, K. S., Jiang, D., Schedin, F., Booth, T., Khotkevich, V., Morozov, S., Two-
1634 dimensional atomic crystals, 2005. *Proceedings of the National Academy of Sciences of the*
1635 *United States of America* 102 (30), 10451-10453.

1636 Obayomi, K. S., Lau, S. Y., Danquah, M., Chiong, T., Takeo, M., 2022. Advances in graphene
1637 oxide based nanobiocatalytic technology for wastewater treatment, *Environmental*
1638 *Nanotechnology, Monitoring & Management*, 17, 100647.

1639 Pal, P., 2018. Treatment and disposal of pharmaceutical wastewater: toward the sustainable
1640 strategy. *Separation & Purification Reviews*, 47(3), 179-198.

1641 Pan, X., Zhao, Y., Liu, S., Korzeniewski, C. L., Wang, S., Fan, Z., 2012. Comparing graphene-
1642 TiO₂ nanowire and graphene-TiO₂ nanoparticle composite photocatalysts, *ACS Applied*
1643 *Materials and Interfaces*, 4(8), 3944-3950.

1644 Paredes, J. I., Villar-Rodil, S., Fernandez-Merino, M. J., Guardia, L., Martinez-Alonso, A.,
1645 Tascon, J. M. D., 2011. Environmentally friendly approaches toward the mass production of
1646 processable graphene from graphite oxide, *J. Mater. Chem.* 21 (2), 298–306.

1647 Park, C.M., Wang, D., Han, J., Heo, J., Su, C., 2019. Evaluation of the colloidal stability and
1648 adsorption performance of reduced graphene oxide-elemental silver/ magnetite nanohybrids
1649 for selected toxic heavy metals in aqueous solutions, *Applied Surface Science*, 471, 8-17.

1650 Patel, H. K., Kalaria, R. K., okhakar, P. H., Mehta, A. A., Patel, H. V., 2022. An application of
1651 bionanotechnology in removal of emerging contaminants from pharmaceutical waste,
1652 *Development in Wastewater Treatment Research and Processes*, 371-384.

1653 Patil, P.M., Mahamuni, P.P., Shadija, P.G., 2019. Conversion of organic biomedical waste into
1654 value added product using green approach. *Environmental Science Pollution Research*,
1655 26, 6696–6705.

1656 Peng, W., Li, H., Liu, Y., Song, Sh., 2017. A review on heavy metal ions adsorption from water
1657 by graphene oxide and its composites. *Journal of Molecular Liquids*, 230, 496–504.

1658 Peng, J., Yan, J., Chen, Q., Jiang, X., Yao, G., Lai, B. 2018. Natural mackinawite catalytic
1659 ozonation for N, N-dimethylacetamide (DMAC) degradation in aqueous solution: Kinetic,
1660 performance, biotoxicity and mechanism. *Chemosphere*, 210, 831-842.

1661 Perera, S. D., Mariano, R. G., Vu, K., Nour, N., Seitz, O., Chabal, Y., Balkus, K. J., 2012.,
1662 Hydrothermal synthesis of graphene-TiO₂ nanotube composites with enhanced
1663 photocatalytic activity, *ACS Catalysis*, 2(6), 949-956.

1664 Pervaiz, E., Farrukh, S., Yang, M. 2022. Catalytic adsorptive removal of toxic compounds from
1665 water using motifs of Ce doped Co₃O₄/RGO nanohybrids. *Cleaner Engineering and*
1666 *Technology*, 7, 100417.

1667 Phoon, B. L., Ong, C. C., Saheed, M. S. M., Show, P. L., Chang, J-S., Ling, T. C., Lami, S. S.,
1668 Juan, J. C. 2020. Conventional and emerging technologies for removal of antibiotics from
1669 Wastewater, *Journal of Hazardous Materials*, 122961.

1670 Pi, Y., Ma, L., Zhao, P., Cao, Y., Gao, H., Wang, C., Li, Q., Dong, S. Sun, J., 2018. Facile green
1671 synthetic graphene-based Co-Fe Prussian blue analogues as an activator of peroxydisulfate
1672 for the degradation of levofloxacin hydrochloride. *Journal of colloid and interface*
1673 *science*, 526, pp.18-27.

1674 Priya, B., Raizada, P., Singh, N., Thakur, P., Singh, P., 2016.. Adsorptional photocatalytic
1675 mineralization of oxytetracycline and ampicillin antibiotics using Bi₂O₃/BiOCl supported on
1676 graphene sand composite and chitosan, *Journal of Colloid and Interface Science*, 479, 271-
1677 283.

1678 Priyadarshini, S. D., Manikandan, S., Kiruthiga, R., Rednam, U., Babu, P. S., Subbaiya, R.,
1679 Karmegam, N., Kim, W., Govarthanam, M., 2022. Graphene oxide-based nanomaterials for
1680 the treatment of pollutants in the aquatic environment: Recent trends and perspectives – A
1681 review, *Environmental Pollution*, 306, 119377.

1682 Qiao, D., Li, Z., Duan, J., He, X. 2020. Adsorption and photocatalytic degradation mechanism of
1683 magnetic graphene oxide/ZnO nanocomposites for tetracycline contaminants. *Chemical*
1684 *Engineering Journal*, 400, 125952.

1685 Qin, Y., Luo, J., Zhao, Y., Yao, C., Li, Y., An, Q., Xiao, Z., Zhai, S., 2022. Dual-wastes derived
1686 biochar with tailored surface features for highly efficient p-nitrophenol adsorption, *Journal of*
1687 *Cleaner Production*, 353, 131571.

1688 Qu, H., Xiao, X., Han, Z., Hu, M., Shen, S., Yang, L., Jia, F., Wang, T., Ye, Z., Sun, W., Wang,
1689 Y., Huang, L., Zhu, Z., Servati, P., Tang, J., Chen, J., 2022. Graphene Oxide Nanofiltration
1690 Membrane Based on Three-Dimensional Size-Controllable Metal–Organic Frameworks
1691 for Water Treatment, *ACS Applied Nano Materials*, 5(4), 5196–5207.

1692 Radmehr, S., Sabzevari, M. H., Ghaedi, M., Azqhandi, M. H. A., Marahel, F., 2021. Adsorption
1693 of nalidixic acid antibiotic using a renewable adsorbent based on Graphene oxide from
1694 simulated wastewater, *Journal of Environmental Chemical Engineering*, 9(5), 105975.

1695 Rajabi, M., Moradi, O., Sillanpää, M., Zare, K., Asiri, A. M., Agarwal, S., Gupta, V. K., 2019.
1696 Removal of toxic chemical ethidium monoazide bromide using graphene oxide:
1697 Thermodynamic and kinetics study, *Journal of Molecular Liquids*, 293, 111484.

1698 Ramalingam, G., Perumal, N., Priya, A. K., Rajendran, S., 2022. A review of graphene-based
1699 semiconductors for photocatalytic degradation of pollutants in wastewater, *Chemosphere*,
1700 300, 134391.

1701 Reddy, Y. V. M., Shin, J. H., Palakollu, V. N., Sravani, B., Choi, C-H., Park, K., Kim, S-K.,
1702 Madhavi, G., Park, J. B., Shetti, N. P., 2022. Strategies, advances, and challenges
1703 associated with the use of graphene-based nanocomposites for electrochemical biosensors,
1704 *Advances in Colloid and Interface Science*, 304, 102664.

1705 Reina, A., Jia, X. T., Ho, J., Nezich, D., Son, H., Bulovic, V., Dresselhaus, M., Kong, J., 2009.
1706 Large area, few-layer graphene films on arbitrary substrates by chemical vapor deposition,
1707 *Nano Letters* 9 (1), 30–35.

1708 Rokuta, E., Hasegawa, Y., Itoh, A., Yamashita, K., Tanaka, T., Otani, S., 1999. Vibrational spectra
1709 of the monolayer films of hexagonal boron nitride and graphite on faceted Ni, *Surface Science*,
1710 427, 97-101.

1711 Rostamian, R. and Behnejad, H., 2016. A comparative adsorption study of sulfamethoxazole onto
1712 graphene and graphene oxide nanosheets through equilibrium, kinetic and thermodynamic
1713 modeling. *Process Safety and Environmental Protection*, 102, 20-29.

1714 Saleh, H. E. D. M. (2016). Introductory chapter: introduction to hazardous waste
1715 management. *Management of Hazardous Wastes*, 1.

1716 Salvatierra, R. V., Souza, V. H. R., Matos, C. F., Oliveira, M. M., Zarbin, A. J. G., 2015. Graphene
1717 chemically synthesized from benzene at liquid–liquid interfaces, *Carbon*, 93, 924-932.

1718 Santos, J. L., Aparicio, I. Alonso, E., 2007. Occurrence and risk assessment of pharmaceutically
1719 active compounds in wastewater treatment plants. A case study: Seville city (Spain), *Environ.*
1720 *Int.*, 33: 596-601.

1721 Santos, E. J., Kaxiras, E., 2013. Electric-field dependence of the effective dielectric constant in
1722 graphene, *Nano Letter*, 13 (3), 898-902.

1723 Saravanan, A., SenthilKumar, P., Srinivasan, S., Jeevanantham, S., Vishnu, M., Amith, K. V.,
1724 Sruthi, R., Saravanan, R., Vo, D-V, N., 2022. Insights on synthesis and applications of
1725 graphene-based materials in wastewater treatment: A review, *Chemosphere*, 298, 134284.

- 1726 Sehar, S., Sher, F., Zhang, S., Khalid, U., Sulejmanović, J., Lima, E. C., 2020. Thermodynamic
1727 and kinetic study of synthesized graphene oxide-CuO nanocomposites: A way forward to
1728 fuel additive and photocatalytic potentials, *Journal of Molecular Liquids*, 313, 113494.
- 1729 Shahzad, A., Mian, A. H., Khan, M. A., Ali, K., & Hamid, T. 2021. The emergence of different
1730 bacterial pathogens in hospital wastewater samples and their antibiotic resistance
1731 pattern. *Materials Circular Economy*, 3(1), 1-8.
- 1732 Shi, W., Wang, Li., Wang, J., Sun, H., Shi, Y., Guo, F., Lu, Y., 2022. Magnetically retrievable
1733 CdS/reduced graphene oxide/ZnFe₂O₄ ternary nanocomposite for self-generated H₂O₂
1734 towards photo-Fenton removal of tetracycline under visible light irradiation, *Separation and
1735 Purification Technology*, 292, 120987.
- 1736 Shin, H. J., Kim, K. K., Benayad, A., Yoon, S-M., Park, H. K., Jung, I-S., Jin, M. H., Jeong, H-
1737 K., Kim, J. M., Choi, J-Y., Lee, Y. H., 2009. Efficient reduction of graphite oxide by sodium
1738 borohydride and its effect on electrical conductance, *Advanced Functional Materials*, 19 (12),
1739 1987-1992.
- 1740 Sohal, B., Bhat, S. A., Vig, A., P., 2021. Vermiremediation and comparative exploration of
1741 physicochemical, growth parameters, nutrients and heavy metals content of biomedical waste
1742 ash via ecosystem engineers *Eisenia fetida*, *Ecotoxicology and Environmental Safety*, 227,
1743 112891.
- 1744 Somasekaran, B., Thirunarayanaswamy, A., Palanivel, I., 2022. Synthesis of Graphene and
1745 fabrication of Aluminium-Gr_p nanocomposites: A review, 50(5), 2436-2442.
- 1746 Song, W., Yang, T., Wang, X., Sun, Y., Ai, Y., Sheng, G., Hayat, T., Wang, X., 2016.
1747 Experimental and theoretical evidence for competitive interactions of tetracycline and
1748 sulfamethazine with reduced graphene oxides. *Environmental Science: Nano*, 3, 1318-1326.
- 1749 Song, D., Mahajan, A., Secor, E. B., Hersam, M. C., Francis, F., Frisbie, C. D., 2017. High-
1750 resolution transfer printing of graphene lines for fully printed, flexible electronics, *ACS Nano*,
1751 11 (7), 7431-7439.
- 1752 Song, C., Guo, B. B., Sun, X. F., Wang, S. G., Li, Y. T. 2019. Enrichment and degradation of
1753 tetracycline using three-dimensional graphene/MnO₂ composites. *Chemical Engineering
1754 Journal*, 358, 1139-1146.
- 1755 Stankovich, S., Dikin, D. A., Piner, R. D., Kohlhaas, K. A., Kleinhammes, A., Jia, Y., 2007. Syn-
1756 thesis of graphene-based nanosheets via chemical reduction of exfoliated graphite oxide,
1757 *Carbon* 45 (7), 1558–1565.
- 1758 Staudenmaier, L., 1898. Verfahren zur darstellung der graphitsäure. *Ber Deutsche Chem. Ges.*
1759 31, 1481-1487.
- 1760 Su, H., Ye, Z., Hmidi, N. 2017. High-performance iron oxide-graphene oxide nanocomposite
1761 adsorbents for arsenic removal. *Colloids and Surfaces A: Physicochemical and Engineering
1762 Aspects*, 522, 161-172.
- 1763 Suksompong, T., Thongmee, S., Sudprasert, W., 2021. Efficacy of a Graphene Oxide/Chitosan
1764 Sponge for Removal of Radioactive Iodine-131 from Aqueous Solutions, *Life*, 11(7), 721.
- 1765 Tabish, S. A., 2005. Ecohealth: management of biomedical waste. *Hospital Infection Control:
1766 Conceptual Framework*. Academia Publishers, 139-145.
- 1767 Tang, H., Ehlert, G. J., Lin, Y., Sodano, H. A., 2011. Highly efficient synthesis of graphene
1768 nanocomposites, *Nano Letters*, 12 (1), 84–90.

- 1769 Tang, Y., Guo, H., Xiao, L., Yu, S., Gao, N., Wang, Y. 2013. Synthesis of reduced graphene
1770 oxide/magnetite composites and investigation of their adsorption performance of
1771 fluoroquinolone antibiotics. *Colloids and Surfaces A: Physicochemical and Engineering*
1772 *Aspects*, 424, 74-80.
- 1773 Tang, Y., Liu, X., Ma, C., Zhou, M., Huo, P., Yu, L., Pan, J., Shi, W., Yan, Y., 2015. Enhanced
1774 photocatalytic degradation of tetracycline antibiotics by reduced graphene oxide CdS/ZnS
1775 heterostructure photocatalysts, *New Journal of Chemistry*, 39, 5150-5160.
- 1776 Tayel, A., Ramadan, A. R., El Seoud, O. A., 2018. Titanium dioxide/graphene and titanium
1777 dioxide/graphene oxide nanocomposites: Synthesis, characterization and photocatalytic
1778 applications for water decontamination, *Catalysts*, 8 (11), 491.
- 1779 Tong, A. Y.C. Peake, B. M. and Braund, R., 2011. Disposal practices for unused medications
1780 around the world. *Environment International*, 37(1), 292–298.
- 1781 Ullah, T., Gul, K., Khan, H., Ara, B., Zia, T. U. H. 2022. Efficient removal of selected
1782 fluoroquinolones from the aqueous environment using reduced magnetic graphene
1783 oxide/polyaniline composite. *Chemosphere*, 133452.
- 1784 Vellinga, A. Cormican, S. Driscoll, J. Furey, M. O'Sullivan, M. and Cormican, M. (2014) Public
1785 practice regarding disposal of unused medicines in Ireland. *M. Sci. Total Environ.*, 478: 98–
1786 102.
- 1787 Verma, S., Nadagouda, M. N. 2021. Graphene-Based Composites for Phosphate Removal. *ACS*
1788 *omega*, 6(6), 4119-4125.
- 1789 Verma, M., Lee, I., Oh, J., Kumar, V., Kim, H., 2022. Synthesis of EDTA-functionalized graphene
1790 oxide-chitosan nanocomposite for simultaneous removal of inorganic and organic pollutants
1791 from complex wastewater *Chemosphere*, 287, 132385.
- 1792 Wang, G., Yang, J., Park, J., Gou, X., Wang, B., Liu, H., 2008. Facile synthesis and
1793 characterization of graphene nanosheets, *Journal of Physical Chemistry C* 112 (22), 8192–
1794 8195.
- 1795 Wang, X. Song, L. Yang, H. Xing, W. Candela, B. Hu, Y. 2012. Simultaneous reduction and
1796 surface functionalization of graphene oxide with POSS for reducing fire hazards in epoxy
1797 composites, *Journal of Material Chemistry*, 22 (41), 22037–22043.
- 1798 Wang, F., Yang, T., Wang, H., Song, Q., Tan, F., Cao, Y., 2016. Removal of ciprofloxacin from
1799 aqueous solution by a magnetic chitosan grafted graphene oxide composite, *Journal of*
1800 *Molecular Liquids*, 222, 188-194.
- 1801 Wang, D., Zhang, G., Zhou, L., Wang, M., Cai, D., Wu, Z., 2017. Synthesis of a multifunctional
1802 graphene oxide-based magnetic nanocomposite for efficient removal of Cr (VI). *Langmuir* 33,
1803 7007-7014.
- 1804 Wang K, Pang J, Li L, Zhou S, Li Y, Zhang T. 2018. Synthesis of hydrophobic carbon
1805 nanotubes/reduced graphene oxide composite films by flashlight irradiation. *Frontiers of*
1806 *Chemical Science and Engineering*, 12(3), 376-82.
- 1807 Wang, K., Wu, J., Zhu, M., Zheng, Y-Z, Tao, X., 2020. Highly effective pH-universal removal of
1808 tetracycline hydrochloride antibiotics by UiO-66-(COOH)₂/GO metal–organic framework
1809 composites, *Journal of Solid State Chemistry*, 284, 121200.
- 1810 Wang, J., Zhang, J., Han, L., Wang, J., Zhu, L., Zeng, H., 2021a. Graphene-based materials for
1811 adsorptive removal of pollutants from water and underlying interaction mechanism,
1812 *Advances in Colloid and Interface Science* 289, 102360.

1813 Wang, J., Li, X., Tang, L., Ma, X., Lu, L., Chen, Y., Zhong, C. 2021b. Synthesis Approaches to
1814 Magnetic Graphene Oxide and Its Application in Water Treatment: A Review. *Water, Air, &*
1815 *Soil Pollution*, 232(8), 1-16.

1816 Wang, J., Zang, L., Wang, L., Tian, Y., Yang, Z., Yue, Y., Sun, L., 2022. Magnetic cobalt
1817 ferrite/reduced graphene oxide (CF/rGO) porous balls for efficient photocatalytic degradation
1818 of oxytetracycline, *Journal of Environmental Chemical Engineering*, 10(5), 108259.

1819 Wu, T., Liu, S., Li, H., Wang, L., Sun, X., 2011. Production of reduced graphene oxide by UV
1820 irradiation, *Journal of Nanoscience and Nanotechnology* 11 (11), 10078–10081.

1821 Wu, S., Zhao, X., Li, Y., Du, Q., Sun, J., Wang, Y., Wang, X., Xia, Y., Wang, Z., Xia, L., 2013.
1822 Adsorption properties of doxorubicin hydrochloride onto graphene oxide: equilibrium, kinetic
1823 and thermodynamic Studies, *Materials*, 6, 2026-2042.

1824 Xiao, R., Wang, S., Ibrahim, M. H., Abdu, H. I., Shan, D., Chen, J., Lu, X. 2019. Three-
1825 dimensional hierarchical frameworks based on molybdenum disulfide-graphene oxide-
1826 supported magnetic nanoparticles for enrichment fluoroquinolone antibiotics in water. *Journal*
1827 *of Chromatography A*, 1593, 1-8.

1828 Xing, H.T., Chen, J.H., Sun, X., Huang, Y.H., Su, Z.B., Hu, S.R., Weng, W., Li, S.X., G H, X.,
1829 2015. NH₂-rich polymer/graphene oxide use as a novel adsorbent for removal of Cu(II) from
1830 aqueous solution. *Chemical Engineering Journal*, 263, 280-289.

1831 Xu, X., Ding, X., Yang, X., Wang, P., Li, S., Lu, Z., Chen, H., 2019. Oxygen vacancy boosted
1832 photocatalytic decomposition of ciprofloxacin over Bi₂MoO₆: Oxygen vacancy engineering,
1833 biotoxicity evaluation and mechanism study, *Journal of Hazardous Material*, 364, 691-699.

1834 Xu, M., Wang, Y., Ha, E., Zhang, H., Li, C., 2021. Reduced graphene oxide/Bi₄O₅Br₂
1835 nanocomposite with synergetic effects on improving adsorption and photocatalytic activity
1836 for the degradation of antibiotics, *Chemosphere*, 265, 129013.

1837 Yakout, A. A., Alshitari, W., Akhdhar, A., 2021. Synergistic effect of Cu-nanoparticles and β-
1838 cyclodextrin functionalized reduced graphene oxide nanocomposite on the adsorptive
1839 remediation of tetracycline antibiotics, *Carbohydrate Polymers*, 273, 118528.

1840 Yashas, S. R., Shivaraju, H. P., McKay, G., Shahmoradi, B., Maleki, A., Yetilmezsoy, K., 2021.
1841 Designing bi-functional silver delafossite bridged graphene oxide interfaces: Insights into
1842 synthesis, characterization, photocatalysis and bactericidal efficiency, , *Chemical Engineering*
1843 *Journal*, 426, 131729.

1844 Yan, J., Li, R., 2022. Simple and low-cost production of magnetite/graphene nanocomposites for
1845 heavy metal ions adsorption, *Science of The Total Environment*, 813, 152604.

1846 Yang, K., Chen, B., Zhu, L. 2015. Graphene-coated materials using silica particles as a framework
1847 for highly efficient removal of aromatic pollutants in water. *Scientific reports*, 5(1), 1-12.

1848 Yang, A., Wang, Z., Zhu, Y. 2021a. Facile preparation and highly efficient sorption of magnetic
1849 composite graphene oxide/Fe₃O₄/GC for uranium removal. *Scientific Reports*, 11(1), 1-10.

1850 Yang, X, Chen, Z., Zhao, W., Liu, C., Qian, X., Zhang, M., Wei, G., Khan, F., Ng, Y. H., Ok,
1851 Y. S., 2021b. Recent advances in photodegradation of antibiotic residues in water, *Chemical*
1852 *Engineering Journal*, 405, 126806.

1853 Yang, L., Xiao, X., Shen, S., Lama, J., Hu, M., Jia, F., Han, Z., Qu, H., Huang, L., Wang, Y.,
1854 Wang, T., Ye, Z., Zhu, Z., Tang, J., Chen, J., **2022**. Recent Advances in Graphene Oxide
1855 Membranes for Nanofiltration, *ACS Applied Nano Materials*, 5(3), 3121–3145.

1856 Yang, J., Shojaei, S., Shojaei, S., 2022. Removal of drugs and dye from aqueous solutions by
1857 graphene oxide: Adsorption studies and chemometrics methods, *npj clean water*, 5(5), 1147.

1858 Yang, P., Yu, F., Yang, Z., Zhang, X., Ma, J., 2022. Graphene oxide modified κ -
1859 carrageenan/sodium alginate double-network hydrogel for effective adsorption of antibiotics
1860 in a batch and fixed-bed column system, *Science of The Total Environment*, 837, 155662.

1861 Yazdi, G. R., Iakimov, T., Yakimova, R., 2016. Epitaxial graphene on silicon carbide: A Review
1862 of Growth and Characterization, *Crystal*, 6, 53.

1863 Yi, M., Shen, Z., 2015. A review on mechanical exfoliation for the scalable production of
1864 graphene, *Journal of Materials Chemistry A*, 3 (22), 11700–11715.

1865 Yu, F., Li, Y., Han, S., Ma, J. 2016. Adsorptive removal of antibiotics from aqueous solution using
1866 carbon materials, *Chemosphere*, 153, 365-385,

1867 Zaied, B. K., Rashid, M., Nasrullah, M., Zularisam, A. W., Pant, D., & Singh, L. (2020). A
1868 comprehensive review on contaminants removal from pharmaceutical wastewater by
1869 electrocoagulation process. *Science of the Total Environment*, 726, 138095.

1870 Zakrzewska-Trznadel, G., 2013. Advances in membrane technologies for the treatment of liquid
1871 radioactive waste. *Desalination*, 321, 119-130.

1872 Zanin, E., Scapinello, J., Oliveira, M.D., Maria, J., Mello, M.D., Antonio, M., Oliveira, J.V., Dal,
1873 J., 2017. Adsorption of heavy metals from wastewater graphic industry using clinoptilolite
1874 zeolite as adsorbent. *Process Safety and Environmental Protection*. 105, 194-200.

1875 Zhang, Y., Small, J. P., Pontius, W. V., Kim, P., 2005. Fabrication and electric-field-dependent
1876 transport measurements of mesoscopic graphite devices, *Applied Physics. Letters*. 86,
1877 073104.

1878 Zhang, X., Jiang, X., Zhang, K., Mao, L., Luo, J., Chi, C., Chan, H. S. O., Wu, J., 2010. Synthesis,
1879 Self-Assembly, and Charge Transporting Property of Contorted Tetrabenzocoronenes, *Journal*
1880 *of Organic Chemistry*, 23, 8069-8077.

1881 Zhang, Y., Jiao, Z., Hu, Y., Lv, S., Fan, H., Zeng, Y., Hu, J., Wang, M., 2017. Removal of
1882 tetracycline and oxytetracycline from water by magnetic Fe₃O₄@graphene, *Environmental*
1883 *Science and Pollution Research*, 24, 2987-2995.

1884 Zhang, R., Li, Y., Cai, Y., Han, Q., Zhang, T., Liu, Y., Zeng, K., Zhao, C., 2020. Photocatalytic
1885 Poly(vinylidene fluoride) membrane of Ag₃PO₄/GO/APTES for water treatment, *Colloids and*
1886 *Surfaces A: Physicochemical and Engineering Aspects*, 597, 124779.

1887 Zhang, Z., Xiao, X., Zhou, Y., Huang, L., Wang, Y., Rong, Q., Han, Z., Qu, H., Zhu, Z., Xu, S.,
1888 Tang, J., Jun Chen, 2021. Bioinspired Graphene Oxide Membranes with pH-Responsive
1889 Nanochannels for High-Performance Nanofiltration *ACS Nano*, 15(8), 13178–13187.

1890 Zhang, Y., Wang, H., Gao, K., Huang, D., Hou, L., Yang, Y., 2022a. Efficient removal of Cs(I)
1891 from water using a novel Prussian blue and graphene oxide modified PVDF membrane:
1892 Preparation, characterization, and mechanism, *Science of The Total Environment*, 838 (4),
1893 156530.

1894 Zhang, N., Ning, X., Chen, J., Xue, J., Lu, G., Qiu, H., 2022b. Photocatalytic degradation of
1895 tetracycline based on the highly reactive interface between graphene nanopore and TiO₂
1896 nanoparticles, *Microporous and Mesoporous Materials*, 338, 111958.

1897 Zheng Q-F, Guo Y, Liang Y, Shen Q. 2020. Graphene nanoribbons from electrostatic-force-
1898 controlled electric unzipping of single-and multi-walled carbon nanotubes. ACS Applied
1899 Nano Materials, 3(5), 4708-16.

1900 Zhou, X., Zhang, J., Wu, H., Yang, H., Zhang, J., Guo, S., 2011. Reducing graphene oxide via
1901 hydroxylamine: a simple and efficient route to graphene, Journal of Physical Chemistry C 115
1902 (24), 11957–11961.

1903 Zhao, Y., Wang, Y., Shi, H., Liu, E., Fan, J., Hu, X., 2018. Enhanced photocatalytic activity of
1904 ZnSe QDs/g-C₃N₄ composite for Ceftriaxone sodium degradation under visible light, Material
1905 Letters, 231, 150-153.

1906 Zhou, L., Alvarez, O.G., Mazon, C.S., Chen, L., Deng, H., Sui, M., 2016. The roles of conjugations
1907 of graphene and Ag in Ag₃PO₄-based photocatalysts for degradation of sulfamethoxazole,
1908 Catalysis Science and Technology, 6, 5972-5981.

1909 Zhou, J., Fang, M., Yang, K., Lu, K., Fei, H., Mu, P., He, R., 2022. MIL-101(Cr)-NH₂/reduced
1910 graphene oxide composite carrier enhanced thermal conductivity and stability of shape-
1911 stabilized phase change materials for thermal energy management, Journal of Energy Storage,
1912 52, 104827.

1913 Zhu, X., Tsang, D.C., Chen, F., Li, S., Yang, X., 2015. Ciprofloxacin adsorption on graphene and
1914 granular activated carbon: kinetics, isotherms, and effects of solution chemistry.
1915 Environmental Technology, 36, 3094-3102.

1916 Zhu, S., Xia, M., Chu, Y., Khan, M. A., Lei, W., Wang, F., Muhmood, T., Wang, A., 2018.
1917 Adsorption and Desorption of Pb(II) on L-Lysine Modified Montmorillonite and the
1918 simulation of Interlayer Structure, Applied Clay Science, 169, 40-47.

1919 Zhu, S., Khan, M. A., Kameda, T., Xu, H., Wang, F., Xia, M., Yoshioka, T., 2022. New insights
1920 into the capture performance and mechanism of hazardous metals Cr³⁺ and Cd²⁺ onto an
1921 effective layered double hydroxide based material, Journal of Hazardous Materials,
1922 426, 128062.

1923 Zou, Y., Walton, A. S., Kinloch, I. A., Dryfe, R. A., 2016. Investigation of the differential
1924 capacitance of highly ordered pyrolytic graphite as a model material of graphene. Langmuir,
1925 32 (44), 11448-11455.

1926 Zou, S-J., Chen, Y-F., Zhang, Y., Wang, X-F., You, N., Fan, H-T., 2021. A hybrid sorbent of α -
1927 iron oxide/reduced graphene oxide: Studies for adsorptive removal of tetracycline antibiotics,
1928 Journal of Alloys and Compounds, 863, 158475.

1929
1930
1931
1932